Ligand Exchange Reactions of Sodium Cation Complexes Examined Using Guided Ion Beam Mass Spectrometry: Relative and Absolute Dissociation Free Energies and Entropies

Jay C. Amicangelo*

School of Science, Penn State Erie, The Behrend College, Station Road, Erie, Pennsylvania 16563

P. B. Armentrout*

Department of Chemistry, University of Utah, Salt Lake City, Utah 84112

Received: July 28, 2004; In Final Form: September 20, 2004

Guided ion beam mass spectrometry is used to study the ligand exchange reactions of Na^+L_1 with L_2, where L_1, $L_2 = H_2O$, C_6H_6, CH_3OH, CH_3OCH_3, NH_3, and C_2H_5OH, as a function of kinetic energy. For the endothermic ligand exchange reactions, reaction endothermicities are obtained by analyzing the kinetic energy dependence of the cross sections using our empirical threshold modeling equation. The thresholds are found to be systematically higher than values previously determined using competitive CID experiments by 0.07–0.2 eV. An analysis of the endothermic cross sections using a bimolecular, polyatomic phase theory model and a competitive, bimolecular RRKM model demonstrates that the systematic deviations result from a competitive shift between the thermoneutral reactions back to the reactants and the endothermic reactions to the ligand exchange products. For all reactions, thermal rate constants, $k(298)$, are determined by modeling the cross sections in the low-energy region and integrating the model over a Maxwell–Boltzmann distribution of relative energies. From the rate constants for the forward and reverse reactions, equilibrium constants and relative free energies at 298 K for the ligand exchange processes are determined. The relative free energies are converted to absolute Na^+-L dissociation free energies, ΔG_{298}, by minimizing the differences with a set of ΔG_{298} values obtained from equilibrium studies using FT-ICR mass spectrometry. Comparisons are made to previous experimental and theoretical absolute Na^+-L dissociation free energies from several sources. Using the absolute Na^+-L dissociation free energies from this work and absolute Na^+-L dissociation enthalpies measured previously in our laboratory, dissociation entropies are determined for the Na^+-L complexes.

Introduction

Recently, there have been several reviews and comprehensive studies regarding the gas-phase thermochemistry (both experimental and theoretical) of sodium cations with small organic molecules.[1–5] The interest in this topic is a result of the importance of the sodium cation in biological systems[6] as well as the increased use of gas-phase sodium cations in biological applications of mass spectrometry.[7] Knowledge of accurate, absolute thermochemistry for sodium cation complexes is necessary for a complete understanding of the participation and binding characteristics of sodium ions in various biological systems. Sodium cation ligand complexes are also good systems to use in exploring the fundamental means of determining accurate thermodynamic information.

We have previously reported accurate Na^+-L bond dissociation energies (BDEs) for $L = H_2O$, C_6H_6, CH_3OH, CH_3OCH_3, NH_3, and C_2H_5OH, determined using competitive collision-induced dissociation (CCID) experiments of doubly ligated sodium cation complexes.[8] This CCID study was undertaken because there was some disagreement in the literature, including previous work from our laboratory, over the absolute and relative bond dissociation energies for the sodium cation to several of these ligands.[3] Most notable were the discrepancies for the relative BDEs of the sodium cation with benzene and water. Early high-pressure mass spectrometry studies[9–11] and more

recent FT-ICR experiments[2] were in qualitative agreement in that both found that the binding energy of Na^+ to benzene is greater than that to water. Quantitatively, however, the binding energies determined from these two studies differed significantly, with an average deviation of approximately 14 kJ/mol. In contrast to these determinations, our previous absolute collision-induced dissociation (CID) studies indicated that Na^+ is more strongly bound to water[12] than to benzene,[3,13] although the uncertainties in these values would allow the opposite conclusion. Using the CCID experiments, we were able to refine our previous absolute binding enthalpies and determine that Na^+ is more strongly bound to benzene than to water by 7.5 ± 3.4 kJ/mol at 0 K. CCID experiments for all of the ligands given above provided binding affinities (enthalpies) to the sodium cation in the order $C_2H_5OH > NH_3 > CH_3OCH_3 > CH_3OH > C_6H_6 > H_2O$. The agreement between the absolute BDEs determined from the CCID experiments and those derived from FT-ICR experiments[2] (which was the most extensive set of literature values) was excellent, with a mean absolute deviation of 0.9 ± 0.5 kJ/mol. There was one feature of this comparison that concerned us: the quantities determined in the FT-ICR experiments were actually Na^+-L dissociation free energies, ΔG_{298}, and in order to compare these values to our Na^+-L bond enthalpies, ΔH_0, we used dissociation entropies and thermal corrections obtained from ab initio-calculated molecular parameters. Therefore, it appeared appropriate to perform a more direct comparison to the FT-ICR dissociation free energies. The

* E-mail: armentrout@chem.utah.edu.

Ligand Exchange Reactions of Na⁺ Complexes

J. Phys. Chem. A, Vol. 108, No. 48, 2004 **10699**

present experiments were undertaken in an effort to determine accurate relative and absolute Na^+-L dissociation free energies for the ligands in question by examining ligand exchange experiments for the sodium cation complexes, $Na^+L_1 + L_2 \leftrightarrow Na^+L_2 + L_1$, using our guided ion beam mass spectrometer. Such experiments may help establish a valuable, alternative means of determining precise thermochemical differences in cation−ligand binding affinities.

In this work, we perform ligand exchange experiments of Na^+L_1 with L_2, where L_1 and L_2 include water, benzene, methanol, dimethyl ether, ammonia, and ethanol, using a tandem guided ion beam mass spectrometer. Cross sections for the ligand exchange reactions in both directions are analyzed using several models to yield direct measurements of the reaction endothermicities and exothermicities. Thermal rate constants, $k(298)$, of the ligand exchange reactions are determined by modeling the cross sections in the low-energy region and integrating the model over a Maxwell−Boltzmann distribution of relative energies. From the rate constants for the forward and reverse reactions, equilibrium constants and relative dissociation free energies at 298 K for the ligand exchange processes are determined. The relative Na^+-L free energies are converted to absolute values by minimizing the deviations with the ΔG_{298} values determined previously by McMahon and Ohanessian.[2] Comparisons are made to previous experimental and theoretical absolute Na^+-L dissociation free energies from several sources.[1−3,8] Using the absolute Na^+-L dissociation free energies from this work and the absolute Na^+-L dissociation enthalpies determined from our previous CCID experiments,[8] experimental dissociation entropies are derived for the Na^+-L complexes.

Experimental Methods

General. The guided ion beam instrument on which these experiments were performed has been described in detail previously.[14−16] Briefly, ions are created in a dc-discharge/flow tube ion source, as described below. After extraction from the source, the ions are accelerated and passed through a magnetic sector for mass analysis. The mass-selected ions are then decelerated to the desired kinetic energy and focused into an octopole ion beam guide. This device uses radio-frequency electric fields to trap the ions in the radial direction and ensure the complete collection of reactant and product ions.[17,18] The current arrangement consists of two consecutive octopole ion guides, having lengths of 22.9 and 63.5 cm, with a distance between them of 1.0 mm. The rf voltage is the same for the two octopoles, but the dc voltage on the second octopole is slightly more negative (by 0.3 V) for the current experiments. The first octopole passes through a gas cell of effective length 8.26 cm that contains the neutral collision partner, Xe here, at a fairly low pressure (0.05−0.2 mTorr). The unreacted parent and product ions drift to the end of the second octopole from which they are extracted, passed through a quadrupole mass filter for mass analysis, and detected with a secondary electron scintillation ion detector using standard pulse-counting techniques. Raw ion intensities are converted to cross sections as described previously.[14] Absolute cross section magnitudes are estimated to be accurate to ±20%, whereas relative cross sections are accurate to ±5%.

Laboratory (lab) energies are converted to center-of-mass (CM) energies using the conversion $E_{CM} = E_{lab}M/(M + m)$, where M and m are the neutral and ion masses, respectively. All energies cited below are in the CM frame unless otherwise noted. The absolute energy scale and corresponding full width

at half-maximum (fwhm) of the ion beam kinetic energy distribution are determined using the octopole as a retarding energy analyzer as described previously.[14] Because the reaction zone and the energy analysis region are physically the same, ambiguities in the energy analysis resulting from contact potentials, space charge effects, and focusing aberrations are minimized.[14] The energy distributions are nearly Gaussian and have typical fwhm values of 0.2−0.4 eV (lab).

It has been shown previously[19−21] that the shape of integral cross sections of ion−molecule reactions is often affected by multiple collisions with the neutral reactant gas, even when the neutral gas pressure is fairly low. Because the presence and magnitude of these pressure effects are difficult to predict, we measured the pressure dependence of all cross sections examined here. Three gas pressures were used, approximately 0.05, 0.10, and 0.20 mTorr, for all of the ligand exchange reactions. In the present systems, we found a slight to marked dependence on the gas pressure in the collision cell. All cross sections shown below and all analyses reported here are for data that have been extrapolated to zero reactant pressure, as described previously,[20] and therefore rigorously represent single-collision conditions.

Ion Source. The sodium cation complexes are formed in a 1-m-long flow tube[15,20] operating at a pressure of 0.6−0.9 Torr with helium flow rates of 6500−8500 sccm. Sodium ions are generated in a continuous dc discharge by argon ion sputtering of a tantalum cathode with a cavity containing sodium metal. Typical operating conditions of the discharge source are 1.8−2.5 kV and 12−22 mA in a flow of roughly 10% argon in helium. Vapors of the ligands are introduced into the flow approximately 50 cm downstream from the dc discharge. The Na^+L complexes are formed by associative reactions of the sodium cations with the neutral ligands and are stabilized by collisions with the surrounding bath gas. The flow conditions used in this ion source provide more than 10^4 collisions with the He buffer gas such that the ions are believed to be thermalized to 300 K both vibrationally and rotationally. We assume that the ions are in their ground electronic states and that their internal energy is well characterized by a Maxwell−Boltzmann distribution of rovibrational states at 300 K. Previous work from this laboratory has shown that these assumptions are generally valid.[19−25] For the systems involving ammonia, $Na^+(ND_3)$ was used as the reactant ion rather than $Na^+(NH_3)$ because the latter species has the same mass as Ar^+, which is also present in the flow tube.

Data Analysis: Endothermic and Exothermic Processes. The threshold regions of the endothermic ligand exchange reaction cross sections are modeled using eq 1

$$\sigma(E) = \sigma_0 \sum_i \frac{g_i(E + E_i - E_0)^n}{E} \tag{1}$$

where σ_0 is an energy-independent scaling factor, E is the relative translational energy of the reactant ion and neutral, E_0 is the CID threshold at 0 K, and the exponent n is an adjustable parameter. The summation is over the rovibrational states of the reactant ion i, where E_i and g_i are the energy and the population ($\Sigma g_i = 1$) of each state, respectively. The populations of rovibrational excited levels are not negligible at 300 K as a result of the many low-frequency modes present in these sodium cation complexes. The relative reactivities of all rovibrational states, as reflected by the parameters σ_0 and n, are assumed to be equivalent. Vibrational frequencies and rotational constants are taken from previous ab initio calculations and scaled appropriately.[3,8,26] The Beyer−Swinehart algorithm[27,28] is used

to evaluate the rovibrational density of states, and the relative populations, g_i, are calculated using a Maxwell−Boltzmann distribution at 300 K. The scaled vibrational frequencies were increased and decreased by 10% to account for the range in scale factors needed to bring the calculated frequencies into agreement with the experimentally determined frequencies as found by Pople and co-workers.[29,30] The uncertainty that this introduces into the analysis is included in the final uncertainties listed for the reaction threshold, E_0, and the other fitting parameters.

The basic form of eq 1 is expected to be appropriate for translationally driven reactions[31] and has been found to reproduce reaction cross sections well for a number of previous studies of both atom−diatom and polyatomic reactions,[32] including CID processes.[3,12,13,21−25,33−39] The model of eq 1 is convoluted with the kinetic energy distribution of the neutral reactant using the treatment of Chantry[40] or of both reactants using formulas developed by Lifshitz et al.[41] The parameters σ_0, n, and E_0 are optimized by performing a nonlinear least-squares analysis of the data. An estimate of the uncertainty associated with the measurement of E_0 is determined from the range of threshold values obtained for different data sets, for variations in the parameter n, for variations associated with the $\pm10\%$ uncertainties in the vibrational frequencies, and for the error in the absolute energy scale, ±0.05 eV (lab).

Because all sources of internal energy are included in the data analysis of eq 1, the thresholds obtained correspond to the minimum energy necessary for reaction, in other words, the 0 K value. This assumption has been tested for several systems.[21−25,37] It has been previously shown that treating all of the energy of the ion (vibrational, rotational, and translational) as capable of coupling with the reaction coordinate leads to reasonable thermochemistry. The 0 K threshold energies for the ligand exchange reactions will equal the 0 K reaction endothermicities as long as there are no activation barriers in excess of the endothermicities. This assumption is generally true for ion−molecule reactions[32] and should be true for the simple ligand exchange reactions examined here.[42]

For reasons discussed below, the cross sections for the endothermic and exothermic ligand exchange reactions are also modeled using a bimolecular, polyatomic phase space theory (PST) method[43,44] and a version of our RRKM competitive threshold analysis method[45] that has been modified for use in bimolecular reactions and where orbital angular momentum is explicitly conserved. The equations needed for both models have recently been detailed for the related case of association reactions.[46,47] Briefly, these models consider the statistical unimolecular decomposition of the bis-ligated $(L_1)Na^+(L_2)$ complex formed by the reaction of $Na^+(L_1)$ with L_2 and Na^+-(L_2) with L_1. These energized molecules have well-characterized energy and rotational angular momentum distributions. In the RRKM method, orbital angular momentum is conserved, whereas PST allows coupling between orbital and rotational angular momentum while conserving the total angular momentum. To ensure that both models correctly account for the potential energy surface of the reaction, the complexation energy of the ion binding to the neutral reactant is included in the modeling.[8] For reactions involving polar neutral molecules, both methods can account for the effect of the dipole moment on the loose transition states assumed in both entrance and exit channels. The bimolecular PST method uses the locked dipole model,[48] using equations outlined elsewhere.[49] The bimolecular RRKM method uses either the locked dipole or the trajectory parametrization model of Su[50] for ion−polar molecule reactions. A key thing to realize about these models compared to eq 1

and its derivatives is that there are no adjustable parameters that control the shapes of the cross sections (such as n). Once the molecular constants of the reactants, products, and intermediate are specified, the only adjustable parameters are the energetics of the competing reactions and, in many cases, a scaling factor to match the absolute magnitude.

The cross sections for the exothermic ligand exchange reactions are modeled using the bimolecular PST and bimolecular RRKM models described above for the endothermic reactions. Although the exothermic cross sections do not have a threshold that can be used to assess thermochemistry, the absolute magnitudes of these cross sections reflect the competition between the loss of the two ligands from the transiently formed bisligated complex. Hence, an analysis of the cross sections for the exothermic ligand exchange reactions using these models in the present systems allows us to assess whether accurate thermochemistry can be obtained.
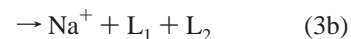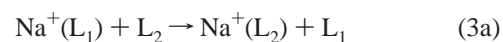
Data Analysis: Thermal Rate Constants. The reaction cross section, $\sigma(E)$, measured in a guided ion beam experiment is related to an energy-dependent rate constant $k(\langle E\rangle)$ by $k(\langle E\rangle) = \sigma(E)v$, where $v = (2E/\mu)^{1/2}$ is the nominal center-of-mass velocity and $\mu = mM/(m + M)$ is the reduced mass of the reactants.[14] The mean relative energy, $\langle E\rangle$, is given by $\langle E\rangle = E + (3/2)\gamma k_BT$, where k_B is the Boltzmann constant, T is the neutral gas temperature, and $\gamma = m/(m + M)$. Thermal (298 K) rate constants are obtained by integrating the cross sections over a Maxwell−Boltzmann distribution of translational energies using eq 2.

$$k(T) = (\pi\mu)^{-1/2}\left(\frac{2}{k_BT}\right)^{3/2}\int_0^\infty \sigma(E)\, E\, \exp\left(-\frac{E}{k_BT}\right)dE \quad (2)$$

Because only the translational energy is varied in these experiments, whereas the internal energies of both reactants are fixed at 298 K, the result is actually the rate as a function of translational temperature. Comparison to a true thermal rate constant is most appropriate at kinetic energies near 298 K (i.e., $(^3/_2)k_BT$ (298 K) = 0.0385 eV). In the determinations of the thermal rate constants for the ligand exchange reactions examined here, the experimental cross sections, $\sigma(E)$, used in eq 2 are represented by a simple power law, $\sigma(E) = \sigma_0E^{-m}$, to model the low-energy portion of the cross sections (maximum energies of 0.1−0.5 eV). Uncertainties in the absolute magnitudes of the thermal rate constants include the absolute uncertainties in the cross sections ($\pm20\%$) and the energy scale (±0.05 eV lab) as well as deviations obtained from analyzing different data sets and variations in the parameters (σ_0 and m) of the power law fits to the low-energy cross sections.

Results and Discussion

Ligand Exchange and Collision-Induced Dissociation Cross Sections. Cross sections were obtained for ligand exchange experiments of $Na^+(L_1)$ with L_2, where L_1 and L_2 include water, benzene, methanol, dimethyl ether, ammonia, and ethanol, in both the forward and reverse directions. These results are shown in Figure 1 for four example systems examined, and the remainder are shown in Figure 1S, available in the Supporting Information. The dominant processes observed for all systems are ligand exchange, reaction 3a, and collision-induced dissociation (CID), reaction 3b.
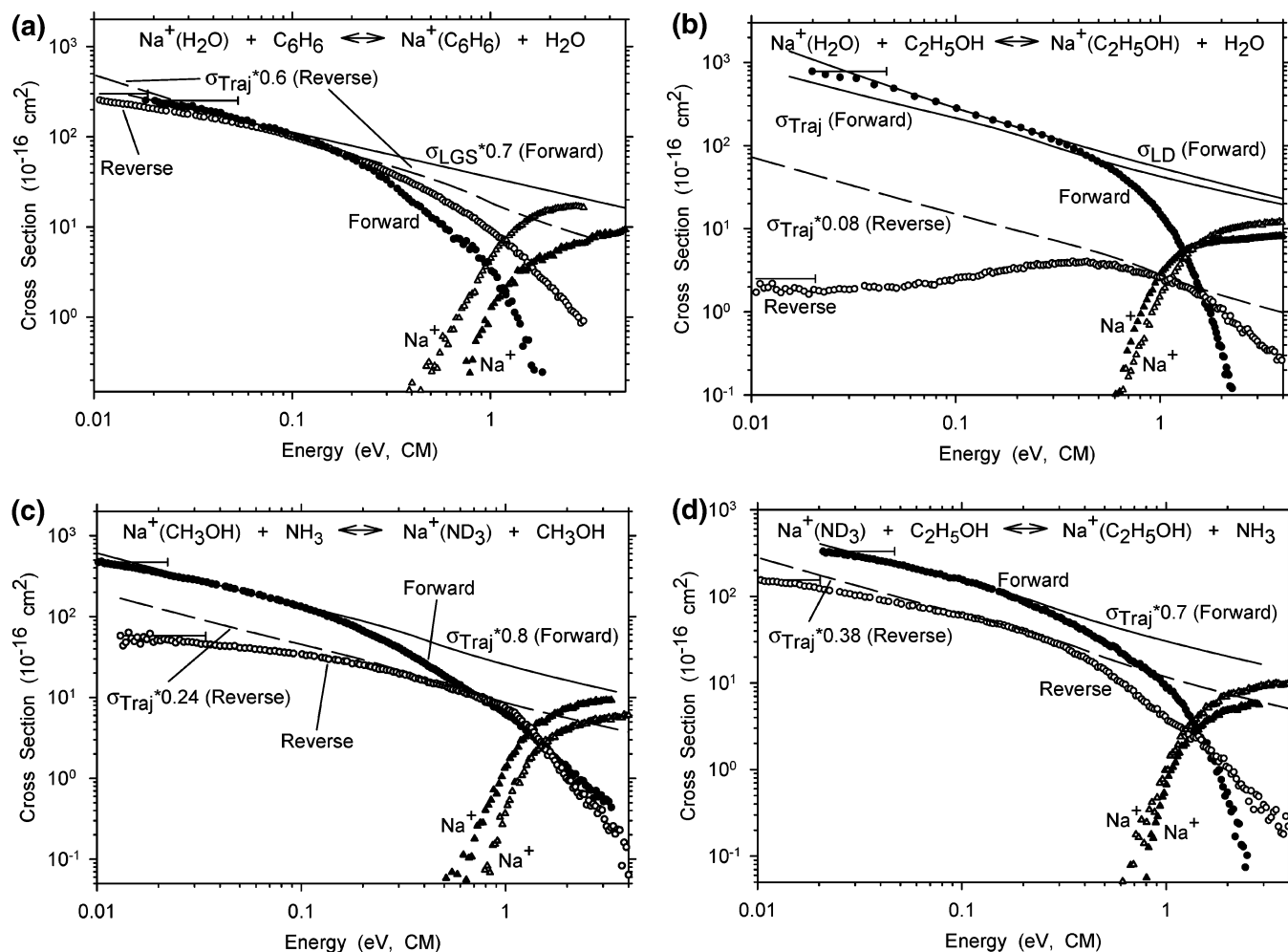
$$Na^+(L_1) + L_2 \rightarrow Na^+(L_2) + L_1 \quad (3a)$$

$$\rightarrow Na^+ + L_1 + L_2 \quad (3b)$$

Ligand Exchange Reactions of Na+ Complexes

J. Phys. Chem. A, Vol. 108, No. 48, 2004 **10701**

Figure 1. Zero-pressure-extrapolated cross sections for the reactions of (a) $Na^+(H_2O)$ with C_6H_6 and $Na^+(C_6H_6)$ with H_2O, (b) $Na^+(H_2O)$ with C_2H_5OH and $Na^+(C_2H_5OH)$ with H_2O, (c) $Na^+(CH_3OH)$ with NH_3 and $Na^+(ND_3)$ with CH_3OH, and (d) $Na^+(ND_3)$ with C_2H_5OH and $Na^+(C_2H_5OH)$ with NH_3 as a function of kinetic energy in the center-of-mass frame. The solid symbols represent data for the forward (exothermic) reaction, and the open symbols represent data for the reverse (endothermic) reaction. The solid and dashed lines display the theoretical collision cross sections predicted by the LGS model, σ_{LGS},[51] the trajectory parametrization model of Su, σ_{Traj},[50] or the locked dipole model, σ_{LD},[48] for the forward and reverse reactions, respectively. In many cases, the collision cross section is multiplied by an arbitrary scaling factor to bring its magnitude into agreement with the data. Uncertainties in the absolute energies are shown for the lowest-energy cross section data point for the ligand exchange reactions.

Complexation, $(L_1)Na^+(L_2)$, and double-exchange products, $Na^+(L_2)_2$, are also observed in these experiments; however, the cross sections for these products are dependent on the pressure, indicating that they were a result of multiple collisions. In all cases, it was explicitly verified that these cross sections extrapolate to zero at zero reactant pressure, a rigorously single-collision condition.

For all systems examined, the ligand exchange reaction is the dominant low-energy process, exhibiting finite cross sections at the lowest energies with magnitudes between approximately 2 and 800 Å^2. For all of the ligand exchange reactions, except the $Na^+(C_2H_5OH) + H_2O \rightarrow Na^+(H_2O) + C_2H_5OH$ reaction, the cross sections decrease with increasing energy, an energy dependence generally attributed to exothermic processes, with energy dependences between $E^{-0.1}$ and $E^{-0.6}$ below approximately 0.5 eV. At higher energies, the decline is more rapid as CID begins to compete with the ligand exchange reactions. Clearly, only half of these ligand exchange reactions can be exothermic, and half must be endothermic. From our previous study of the CCID of doubly ligated sodium cation complexes with the same ligands,[8] the absolute Na^+-L bond energies are known for these ligands; therefore, it is known which reactions

are actually endothermic in terms of bond enthalpy differences. The reason that most of the cross sections for the endothermic reactions have dependences that appear to be barrierless is due to the internal energy of the reactants. Using molecular parameters determined at the MP2(full)/6-31G(d) level,[3,8,26] we calculate that the average internal energy (vibrational + rotational) at room temperature for the reactants of the endothermic reactions is between 0.12 and 0.19 eV. These energies generally exceed the reaction endothermicities, which range from 0.02 to 0.21 eV (298 K values).[8] Therefore, most of the reactants have enough internal energy to overcome the endothermicity of the reaction and react with high probability (i.e., high cross section magnitude) at low energies.

As mentioned above, the $Na^+(C_2H_5OH) + H_2O \rightarrow Na^+(H_2O) + C_2H_5OH$ reaction, Figure 1b, is the only reaction to display an energy dependence that is obviously endothermic. It has a cross section that rises from $\sim$2 Å^2 at the lowest energies to a maximum of $\sim$4 Å^2 between 0.3 and 0.5 eV and then declines at energies higher than 0.5 eV, as competition with CID begins. This reaction is the most endothermic reaction studied ($E_0 = 0.21$ eV) and the only one where the average internal energy of the reactants (0.17 eV) is smaller than the reaction endother-

TABLE 1: Reaction Enthalpies at 298 K Determined by CCID (kJ/mol), Reaction Free Energies at 298 K Determined by FT-ICR Experiments (kJ/mol), and Exothermic and Endothermic Cross Section Magnitude Scaling Factors (SF) as Compared to Theory[a]

reaction	$|\Delta_r H_{298}|$[b]	$|\Delta_r G_{298}|$[c]	exo SF[d]	endo SF low E[e]	endo SF high E[f]
$Na^+(H_2O) + C_6H_6$	6 (4)	0.0 (0.4)	0.7 (0.1)		
$Na^+(C_6H_6) + H_2O$				0.31 (0.06)	0.6 (0.1)
$Na^+(H_2O) + CH_3OCH_3$	10 (4)	7.9 (0.8)	1.0 (0.2)		
$Na^+(CH_3OCH_3) + H_2O$				0.026 (0.005)	0.15 (0.03)
$Na^+(H_2O) + C_2H_5OH$	20 (4)	14 (1)	1.0 (0.2)		
$Na^+(C_2H_5OH) + H_2O$				0.003 (0.006)	0.08 (0.02)
$Na^+(C_6H_6) + CH_3OH$	2 (3)	6.7 (0.6)	1.0 (0.2)		
$Na^+(CH_3OH) + C_6H_6$				0.10 (0.02)	0.14 (0.03)
$Na^+(CH_3OH) + CH_3OCH_3$	3 (2)	1.2 (0.4)	0.8 (0.2)		
$Na^+(CH_3OCH_3) + CH_3OH$				0.27 (0.05)	0.42 (0.08)
$Na^+(CH_3OH) + NH_3$	7 (2)	5.4 (0.6)	0.8 (0.2)		
$Na^+(ND_3) + CH_3OH$[g]				0.08 (0.02)	0.24 (0.05)
$Na^+(CH_3OCH_3) + NH_3$	5 (2)	4.2 (0.4)	0.7 (0.1)		
$Na^+(ND_3) + CH_3OCH_3$[g]				0.17 (0.03)	0.28 (0.06)
$Na^+(ND_3) + C_2H_5OH$[g]	5 (2)	1.7 (0.6)	0.7 (0.1)		
$Na^+(C_2H_5OH) + NH_3$				0.22 (0.04)	0.38 (0.08)

[a] Uncertainties in parentheses. [b] Absolute magnitude of relative 298 K enthalpy differences determined by CCID experiments.[8] [c] Absolute magnitude of relative 298 K dissociation free energies determined by FT-ICR ligand exchange experiments.[2] [d] Scaling factor for comparing the theoretical collision cross section to the observed exothermic ligand exchange cross section. [e] Scaling factor for comparing the theoretical collision cross section to the observed endothermic ligand exchange cross section at low energies (<0.1 eV). [f] Scaling factor for comparing the theoretical collision cross section to the observed endothermic ligand exchange cross section at high energies (0.1–2.0 eV). [g] $|\Delta_r H_{298}|$ and $|\Delta_r G_{298}|$ values are for the perprotio species.

micity. The small difference in these energies and the fact that the internal energy and kinetic energy of the reactants are broad distributions account for the finite cross section magnitude of this reaction at the lowest energies.

Even though typical endothermic energy dependences of the cross sections are not realized for most of the endothermic reactions examined, the relative energetics of a particular pair of ligands is qualitatively reflected in the cross section magnitudes at low energies. Thus, the endothermic reaction exhibits a finite cross section magnitude that is generally a factor of 2 or more smaller than that of the reverse exothermic reaction at the lowest energies. The exception to this is the $Na^+(H_2O) + C_6H_6 \leftrightarrow Na^+(C_6H_6) + H_2O$ system (Figure 1a). For the C_6H_6 and H_2O ligands, our previous CCID study obtained a Na^+-L bond energy difference of $\Delta_r H_{298} = 6 \pm 4$ kJ/mol (298 K value, Table 1), with C_6H_6 being the more strongly bound ligand.[8] The cross sections for these two reactions, however, display nearly equal magnitudes at the lowest energies. Because the cross section is directly proportional to a rate constant, the low-energy rate constants for these two reactions are similar in magnitude. This actually reproduces the results of McMahon and Ohanessian,[2] who measured a relative 298 K Na^+-L dissociation free energy, $\Delta_r G_{298}$, for these two ligands of 0.0 ± 0.4 kJ/mol (Table 1); therefore, the value of the equilibrium constant for ligand exchange in this system is $K_{LE} = 1.0 \pm 0.2$. It is worth noting that of the ligands studied here the C_6H_6 and H_2O ligands are the only ones for which the dissociation free energies are essentially equal. Therefore, for all other ligand exchange reactions examined, the qualitative trends in terms of relative bond energies are displayed in the cross section magnitudes.

Collision-induced dissociation is also observed and is the dominant process at energies higher than ~2 eV in these systems. The apparent thresholds for CID range from 0.4 to 0.9 eV, and the cross section magnitudes exhibit maxima between 5 and 20 Å². Because our most accurate bond energies for these Na^+-L complexes have already been determined using CCID experiments,[8] the CID cross sections observed in the current experiments will not be discussed further. However, it is worth noting that the thresholds obtained from the current CID processes are generally in agreement with the values determined from our previous direct CID measurements.[3]

Comparison with the Theoretical Collision Cross Section. The ligand exchange cross sections can be compared to models for the collision cross section for ion–molecule reactions. For the reactions with C_6H_6, the Langevin–Gioumousis–Stevenson (LGS)[51] model for nonpolar ion–molecule reactions is used. This is given by $\sigma_{LGS} = e(\pi\alpha/\epsilon_0 E)^{1/2}$, where e is the electron charge, α is the polarizability volume of C_6H_6 (9.9 Å³),[52] ϵ_0 is the vacuum permittivity, and E is the relative kinetic energy of the reactants. For reactions with all other ligands, the trajectory (Traj) parametrization model of Su for ion–polar molecule reactions is used for comparison.[50] For the $Na^+(H_2O) + C_2H_5OH \rightarrow Na^+(C_2H_5OH) + H_2O$ reaction, the locked dipole (LD) model,[48] $\sigma_{LD} = \sigma_{LGS} + e\mu_D/4\epsilon_0 E$, where μ_D is the dipole moment of the neutral molecule, was also used for comparison because the cross section was larger than that predicted by the trajectory parametrization at low energies. Both models depend on the polarizability[52,53] and the dipole moment[52,54] of the neutral molecule. These models are plotted with the data in Figures 1 and 1S after scaling by arbitrary factors that allow a convenient comparison of the energy dependences of the experimental and theoretical cross sections.

All of the exothermic reactions (forward reactions in Figures 1 and 1S) are generally found to follow the energy dependence of the collision cross section in the low-energy region (below 0.3 eV). It is worth noting that the small deviations from the theoretical energy dependences at the lowest energies in some of the cross sections are most likely a result of errors in the absolute energies (±0.05 eV lab). The magnitudes of the cross sections for three of the exothermic reactions (Figures 1c, 1Sa, and 1Sb) are found to be approximately equal to the collision cross section at low energies. For the remaining exothermic reactions, the magnitudes vary between 70 and 80% of the theoretical collision cross section magnitude. Just as described above for the magnitudes of the cross sections for the C_6H_6/H_2O reaction system, the changes in the cross section magnitudes as compared to theory can best be understood in terms of the relative dissociation free energies[2] rather than the relative bond enthalpies for these ligands (Table 1).[8] The three reactions
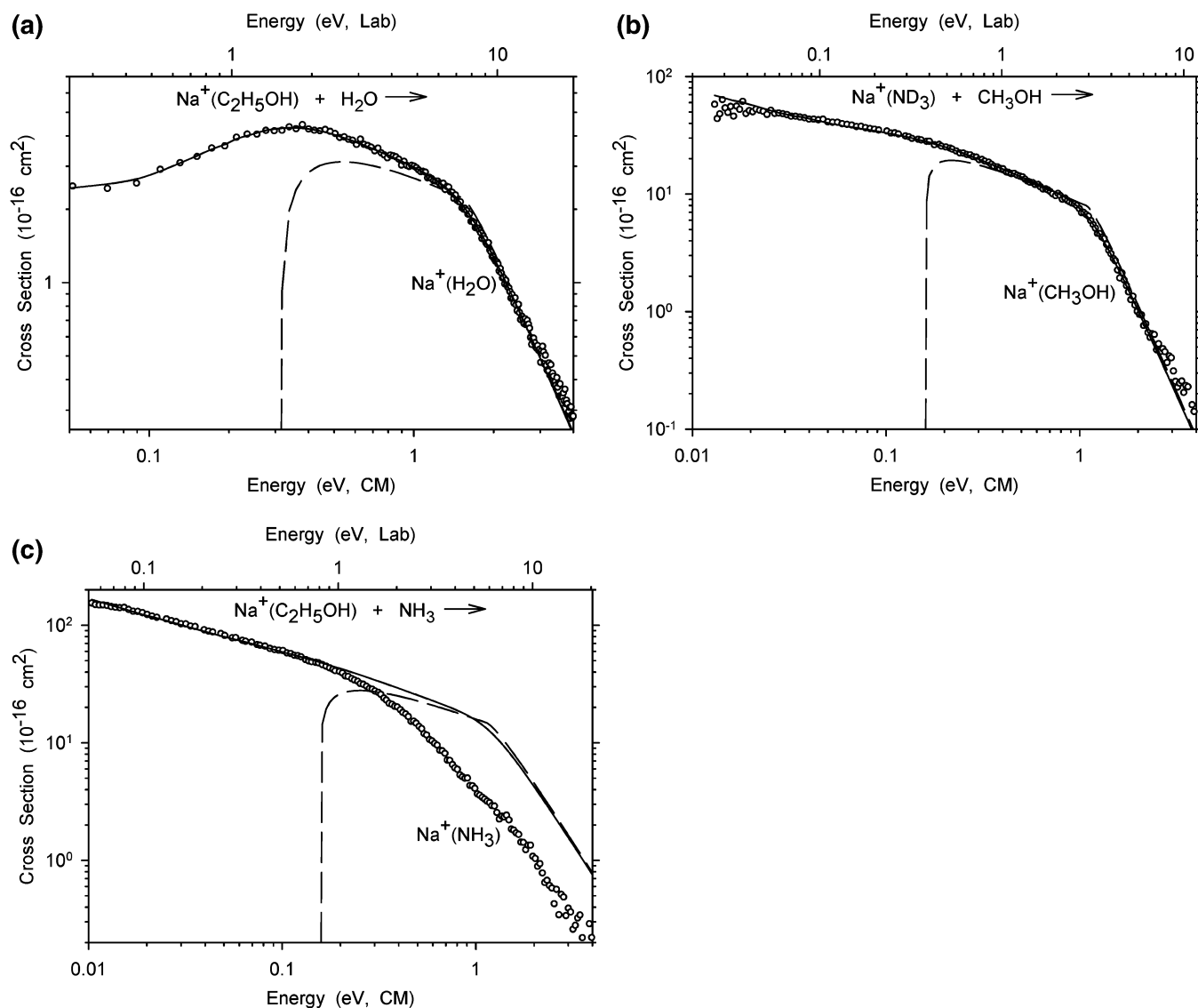
Ligand Exchange Reactions of Na$^+$ Complexes

J. Phys. Chem. A, Vol. 108, No. 48, 2004 **10703**

(a)

(b)

(c)

Figure 2. Zero-pressure-extrapolated cross sections for the endothermic ligand exchange reactions of (a) Na$^+$(C$_2$H$_5$OH) with H$_2$O, (b) Na$^+$(ND$_3$) with CH$_3$OH, and (c) Na$^+$(C$_2$H$_5$OH) with NH$_3$ as a function of kinetic energy in the center-of-mass frame (lower axis) and the laboratory frame (upper axis). Solid lines show the best fits to the data using the model of eq 1, including the high-energy dissociation behavior, convoluted over the neutral and ion kinetic energies and the internal energy distributions of the reactants. Dashed lines show the model cross sections in the absence of experimental kinetic energy broadening for reactants with an internal energy of 0 K.

that have magnitudes approximately equal to the collision cross section, Na$^+$(H$_2$O) + C$_2$H$_5$OH → Na$^+$(C$_2$H$_5$OH) + H$_2$O, Na$^+$(H$_2$O) + CH$_3$OCH$_3$ → Na$^+$(CH$_3$OCH$_3$) + H$_2$O, and Na$^+$(C$_6$H$_6$) + CH$_3$OH → Na$^+$(CH$_3$OH) + C$_6$H$_6$, have the largest free-energy differences, 14 ± 1, 7.9 ± 0.8, and 6.7 ± 0.6 kJ/mol, respectively. The other five exothermic reactions, which all have cross section magnitudes that are less than the collision cross section, have free-energy differences of less than ∼5 kJ/mol. If one compares the magnitude trends in terms of the *enthalpy* differences, then there are clearly some inconsistencies, most notably for Na$^+$(C$_6$H$_6$) + CH$_3$OH → Na$^+$(CH$_3$OH) + C$_6$H$_6$.

The endothermic reactions (reverse reactions in Figures 1 and 1S) can also be compared to the theoretical cross section models. Most of the cross sections for these reactions have larger deviations from the collision cross section at thermal energies (∼0.04 eV) than is observed for the exothermic reactions, with magnitudes ranging from 0.3 to 31% of the collision cross section. At higher energies (0.1−2.0 eV), the cross sections have energy dependences that are similar to the predicted collision

cross sections but with magnitudes of 8−60%. The lower magnitudes observed for these reactions confirm that these are the endothermic reactions of the ligand exchange processes. Similar to that observed for the exothermic reactions, the variations of the endothermic cross section magnitudes generally track better with the relative free energies than with the relative bond enthalpies, as can be seen in Table 1.

Analysis of Endothermic Reactions. Even though the cross sections for the endothermic ligand exchange reactions do not display typical endothermic energy dependences, it was still possible to analyze the cross sections using eq 1.[55] In these cases, the threshold energy is equal to the difference in the bond energies of the two ligands to Na$^+$ (i.e., E_0(Na$^+$L$_1$ + L$_2$ → Na$^+$L$_2$ + L$_1$) = D_0(Na$^+$−L$_1$) − D_0(Na$^+$−L$_2$)). Representative fits using eq 1 for the Na$^+$(C$_2$H$_5$OH) + H$_2$O → Na$^+$(H$_2$O) + C$_2$H$_5$OH, Na$^+$(ND$_3$) + CH$_3$OH → Na$^+$(CH$_3$OH) + ND$_3$, and Na$^+$(C$_2$H$_5$OH) + NH$_3$ → Na$^+$(NH$_3$) + C$_2$H$_5$OH reactions are shown in Figure 2. The fits for all other endothermic ligand exchange reactions are given in Figure 2S, available in the Supporting Information. For five of the reactions (Figures 2a

TABLE 2: Parameters Used in Equation 1 to Model the Endothermic Ligand Exchange (LE) Reactions, Threshold Energies at 0 K, and Reaction Endothermicities Obtained Using Relative Bond Dissociation Energies at 0 K Determined by CCID[a]

reaction	σ_0	n	LE E_0 vib + rot	LE E_0 vib only	ΔE_0 CCID[b]
$Na^+(C_6H_6) + H_2O$	40 (10)	0.6 (0.2)	0.14 (0.07)	0.07 (0.07)	0.08 (0.03)
$Na^+(CH_3OCH_3) + H_2O$	5 (1)	0.3 (0.1)	0.25 (0.04)	0.17 (0.04)	0.13 (0.03)
$Na^+(C_2H_5OH) + H_2O$	3.1 (0.2)	0.4 (0.1)	0.32 (0.04)	0.23 (0.04)	0.23 (0.03)
$Na^+(CH_3OH) + C_6H_6$	5.9 (0.9)	0.3 (0.1)	0.22 (0.05)	0.13 (0.05)	0.02 (0.02)
$Na^+(CH_3OCH_3) + CH_3OH$	30 (10)	0.4 (0.1)	0.16 (0.05)	0.09 (0.05)	0.03 (0.01)
$Na^+(ND_3) + CH_3OH$	10 (1)	0.4 (0.1)	0.14 (0.04)	0.06 (0.04)	0.07 (0.01)[c]
$Na^+(ND_3) + CH_3OCH_3$	15 (5)	0.5 (0.2)	0.12 (0.06)	0.05 (0.06)	0.03 (0.01)[c]
$Na^+(C_2H_5OH) + NH_3$	20 (9)	0.4 (0.2)	0.16 (0.06)	0.08 (0.06)	0.08 (0.01)
MAD[d]			0.10 (0.05)	0.03 (0.04)	

[a] Uncertainties in parentheses. [b] Relative bond dissociation energies determined by CCID experiments[8] [c] Values have been corrected to the values for $Na^+(ND_3)$ as the reactant using zero-point energy differences of the deuterated and perprotio products and reactants (0.017 eV). [d] Mean absolute deviation from CCID relative bond dissociation energies.

and b, 2Sb, 2Sc, and 2Se), the model of eq 1 reproduces the data very well over a fairly extended range of energies (∼2−4 eV) with parameters given in Table 2. These fits use a variation of eq 1 that incorporates a simple statistical model for the high-energy dissociation of the ligand exchange products (beginning near 1 eV).[56] This high-energy model is controlled by two parameters: the BDE of the reactant Na^+-L ion and p, which controls how rapidly the cross section declines above this energy. Here, the BDE that is used is fixed at the absolute Na^+-L BDE determined from our CCID experiments.[8] For the other three reactions (Figures 2c, 2Sa, and 2Sd), the model could fit only the low-energy portions of the cross sections below ∼0.4 eV, unless the reactant Na^+-L ion BDEs that control the decline at high energies were lowered ∼0.5−0.8 eV from the CCID values. An example of the failure of the high-energy model is shown in Figure 2c for the $Na^+(C_2H_5OH) + NH_3 \rightarrow Na^+(NH_3) + C_2H_5OH$ reaction system. Clearly, the model reproduces the data in the low-energy region (below ∼0.2 eV) quite well using the parameters listed in Table 2; however, the cross section begins to decline rapidly at a lower energy than that predicted by the high-energy model. The three systems for which this model failed have the lowest reaction free energies of all of the reactions studied here (Table 1). This is an indication that the close competition between forming products and returning to reactants (controlled by the enthalpic and the entropic factors for these systems) causes our simple model to fail at moderate and higher energies. Regardless, the results of the analysis of all of the endothermic reactions are listed in Table 2 along with the relative bond energies determined from CCID experiments.[8]

The values determined from the analysis of the current ligand exchange cross sections are systematically higher than the values determined from the CCID experiments by 0.06−0.20 eV, with a mean absolute deviation (MAD) of 0.10 ± 0.05 eV (eight values). This type of systematic deviation was observed by Ervin and co-workers (deviations of 0.05−0.09 eV and a MAD of 0.06 ± 0.01 eV; five values), in their examination of bimolecular proton-transfer reactions $F^- + ROH \rightarrow HF + RO^-$.[57] Empirically, these authors found that if the data were analyzed without the inclusion of the rotational energy of the alcohols then the agreement with the literature values was improved. The data in the current ligand exchange reactions were also analyzed without the inclusion of the rotational energy of the reactants, and the results of this type of analysis are also presented in Table 2. Removing the rotational energy improves the agreement between the ligand exchange thresholds and the CCID relative BDEs, with deviations ranging from −0.01 to 0.11 eV and a MAD of 0.03 ± 0.04 eV (eight values). This improvement could be fortuitous because as pointed out by Ervin and co-workers there is no firm basis for the exclusion of rotational energy in these

types of reactions. In fact, previous work from this laboratory on the reactions of N^+ and C^+ with H_2 has demonstrated that rotational energy is available for some reactions.[58,59]

Analysis of Endothermic Reactions Including Competition. A more likely explanation for the high reaction thresholds is a competitive shift. This idea recognizes that the ionic and neutral reactants come together and form a transient energized molecule, the doubly ligated sodium ion. This energized molecule can then dissociate along two competitive pathways— thermoneutral loss back to the original reactants (unobserved dark channel) or endothermic loss to the ligand exchange products. In analyzing the data for this type of competitive shift, we used the bimolecular PST and RRKM models described above.[46] To determine the importance of the dipole moment in the long-range potential, the data are analyzed both with (locked dipole, LD, and trajectory parametrization, Traj, models) and without (Langevin−Gioumousis−Stevenson, LGS, model) the inclusion of the dipole moment. Although the only adjustable parameter in these models could be the reaction energetics, it was found that for the endothermic reactions a scaling factor (σ_0) was needed to obtain calculated cross sections that reasonably fit the shapes and magnitudes of the experimental cross sections. When the scaling factor was fixed at a value of 1.0 and the energetics was adjusted to get the magnitude of the calculated cross sections close to the experimental data, the shape of the calculated cross section did not resemble the experimental cross sections very well. When one considers that the energy dependence of the cross section is more important than the absolute magnitude in determining the energetics of endothermic reactions, it is reasonable to allow a scaling factor in the analysis, which may compensate for some unspecified kinetic parameters. Therefore, analyses for all of the endothermic reactions allowed for the optimization of the scaling factor, and a range of 0.1 to 6.8 was obtained.

The results of analyzing the data using the various versions of the two methods are given in Table 3. Representative fits obtained by using the bimolecular PST (LD and LGS) methods and the bimolecular RRKM (Traj) methods are displayed in Figure 3 for the $Na^+(C_2H_5OH) + H_2O \rightarrow Na^+(H_2O) + C_2H_5OH$, $Na^+(ND_3) + CH_3OH \rightarrow Na^+(CH_3OH) + ND_3$, and $Na^+(C_2H_5OH) + NH_3 \rightarrow Na^+(NH_3) + C_2H_5OH$ reactions. The fits using the RRKM (LD and LGS) methods are, in general, very similar to the fits using the PST (LGS) method and therefore are not displayed explicitly in Figure 3 but rather are given in Figures 5S and 7S, respectively, available in the Supporting Information. For all other endothermic ligand exchange reactions, the fits using the PST (LD and LGS) methods are given in Figures 3S and 4S, respectively, and the fits using the RRKM (LD, Traj, and LGS) methods are given

Ligand Exchange Reactions of Na$^+$ Complexes

J. Phys. Chem. A, Vol. 108, No. 48, 2004 **10705**

TABLE 3: Reaction Endothermicities Obtained Using Phase Space Theory, Bimolecular RRKM Theory, and Relative Bond Dissociation Energies at 0 K Determined by CCID[a]

reaction	ΔE_0					
	PST (LD)[b]	PST (LGS)[c]	RRKM (LD)[d]	RRKM (Traj)[e]	RRKM (LGS)[f]	CCID[g]
Na$^+$(C$_6$H$_6$) + H$_2$O	0.10 (0.04)	0.06 (0.03)	0.07 (0.02)	0.07 (0.03)	0.05 (0.02)	0.08 (0.03)
Na$^+$(CH$_3$OCH$_3$) + H$_2$O	0.07 (0.02)	0.06 (0.03)	0.06 (0.02)	0.06 (0.02)	0.06 (0.03)	0.13 (0.03)
Na$^+$(C$_2$H$_5$OH) + H$_2$O	0.16 (0.02)	0.14 (0.02)	0.16 (0.02)	0.15 (0.02)	0.15 (0.02)	0.23 (0.03)
Na$^+$(CH$_3$OH) + C$_6$H$_6$	0.02 (0.03)	0.05 (0.03)	0.09 (0.03)	0.09 (0.03)	0.05 (0.03)	0.02 (0.02)
Na$^+$(CH$_3$OCH$_3$) + CH$_3$OH	0.06 (0.02)	0.02 (0.03)	0.03 (0.02)	0.02 (0.02)	0.01 (0.03)	0.03 (0.01)
Na$^+$(ND$_3$) + CH$_3$OH	0.06 (0.02)	0.04 (0.02)	0.06 (0.02)	0.05 (0.02)	0.05 (0.02)	0.07 (0.01)[h]
Na$^+$(ND$_3$) + CH$_3$OCH$_3$	0.05 (0.03)	0.04 (0.03)	0.05 (0.03)	0.04 (0.03)	0.04 (0.03)	0.03 (0.01)[h]
Na$^+$(C$_2$H$_5$OH) + NH$_3$	0.07 (0.03)	0.04 (0.03)	0.06 (0.03)	0.04 (0.02)	0.03 (0.03)	0.08 (0.01)
MAD[i]	0.03 (0.03)	0.04 (0.03)	0.03 (0.03)	0.04 (0.03)	0.04 (0.03)	

[a] Uncertainties in parentheses. [b] Analyzed using a bimolecular phase space theory method with the locked dipole model. [c] Analyzed using a bimolecular phase space theory method with the LGS model (no dipole). [d] Analyzed using a bimolecular RRKM method with the locked dipole model. [e] Analyzed using a bimolecular RRKM method with the trajectory parametrization model. [f] Analyzed using a bimolecular RRKM method with the LGS model (no dipole). [g] Relative bond dissociation energies determined by CCID experiments.[8] [h] Values have been corrected to the values for Na$^+$(ND$_3$) as the reactant using zero-point energy differences of the deuterated and perprotio products and reactants (0.017 eV). [i] Mean absolute deviation from CCID relative bond dissociation energies.

in Figures 5S, 6S, and 7S, respectively, available in the Supporting Information.

For most reactions, the range of energies over which the bimolecular PST and RRKM methods reproduced the data was fairly small (0.1−0.4 eV); however, there were several systems for which the methods reproduced the data over a larger energy range (0.6−1.5 eV). The range of energies over which these methods reproduce the data appears to be related to the range of energies over which the experimental cross sections follow the scaled theoretical LD, Traj, and LGS collision cross sections. The significance of the deviations of the PST and RRKM fits from the data at the lowest energies is difficult to assess because this region is the hardest to measure experimentally and is subject to larger errors in both the energy scale and cross section scale than higher energies. Qualitatively, the fits using the various methods are comparable to one another; however, there do appear to be some small differences between them, which can be seen in Figure 3. For the PST method, the LD and LGS models both fit the data over similar ranges of energy; however, the LGS model generally allows the data to be modeled to a lower absolute energy than the LD model. For the RRKM method, the Traj and LGS models generally fit the data over similar ranges of energy and appear to fit over slightly larger energy ranges than the LD model for many systems. Similar to that observed for the PST method, the RRKM (LGS) method seems to allow modeling to a lower absolute energy than the RRKM (LD or Traj) methods. For several reactions, the RRKM (Traj) method does give slightly better fits over intermediate absolute energies than either the RRKM (LD) or RRKM (LGS) method.
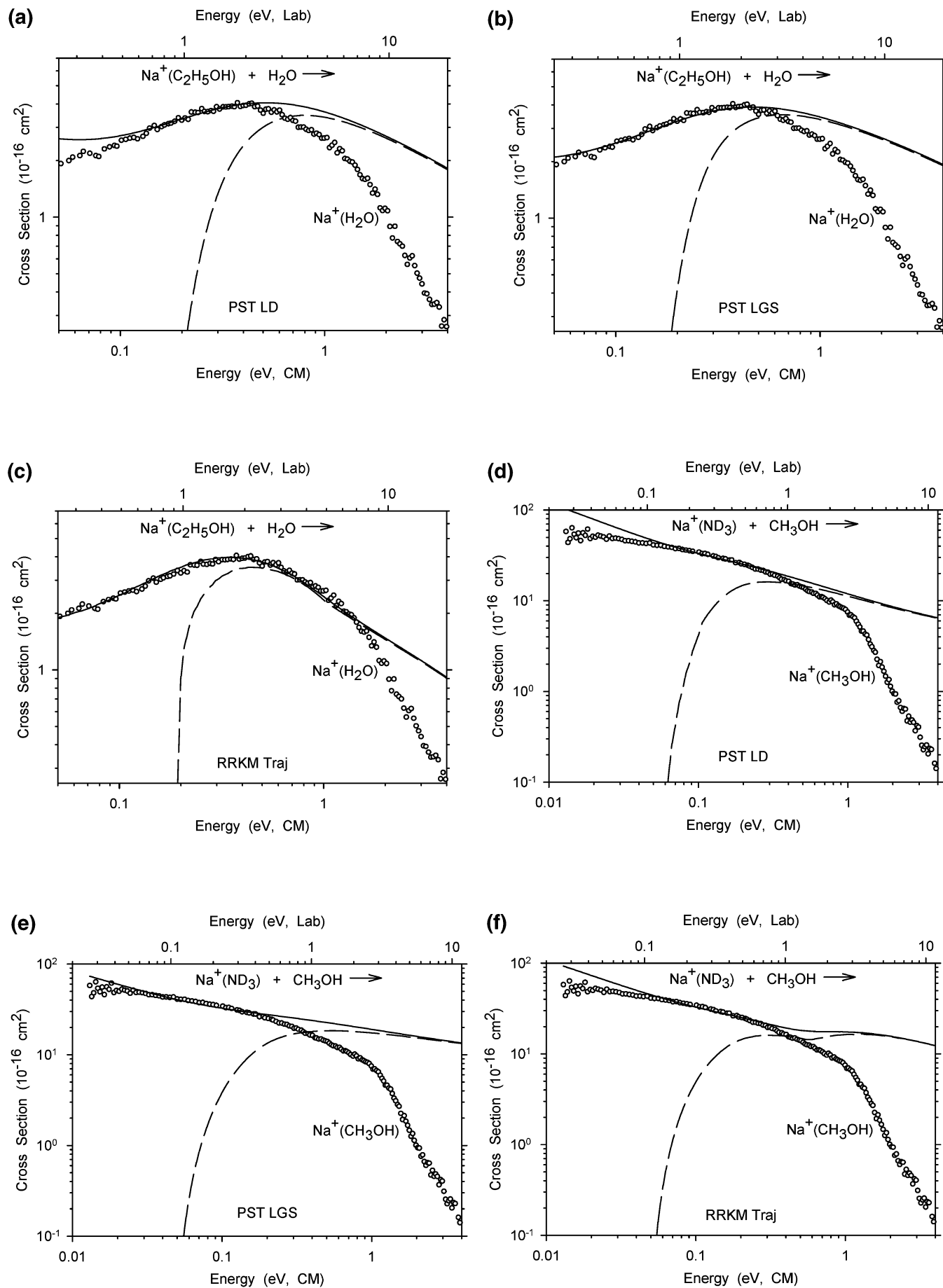
In several systems (e.g., the Na$^+$(ND$_3$) + CH$_3$OH → Na$^+$(CH$_3$OH) + ND$_3$ reaction), the RRKM fits exhibit large increases in the predicted cross sections at elevated energies, with the increases being largest for the LGS model and smallest for the LD model. This has been commented on previously[46] and is the result of the presumption in the RRKM treatment that the orbital angular momentum is conserved throughout the reaction. For certain combinations of reduced masses (specifically when the reduced mass of the ligand exchange products is less than that of the reactants), the (L$_1$)Na$^+$(L$_2$) complex gets trapped behind the centrifugal barrier, thereby leading it to dissociate preferentially by the pathway having the lower reduced mass. In PST, coupling of the orbital and rotational angular momenta allows such "trapped" complexes to reduce their orbital angular momentum, thereby allowing dissociation

back to reactants. This avoids the unrealistic increases seen at elevated energies in the RRKM modeling, which may also influence the predicted cross sections in other systems as well, even though the results are less obvious.

As can be seen from Table 3, the general agreement of the reaction endothermicities determined from the various versions of the PST (LD and LGS) and the RRKM analyses (LD, Traj, and LGS) with the CCID relative BDEs is excellent, with MADs for eight values of 0.03 ± 0.03, 0.04 ± 0.03, 0.03 ± 0.03, 0.04 ± 0.03, and 0.04 ± 0.03 eV, respectively. Comparing the LGS results with the LD and Traj results for both the PST and RRKM methods, it can be seen that the endothermicities obtained without including the dipole (LGS model) are slightly lower than the other results for most systems. Also, comparing the LD and Traj results for the RRKM method, the latter endothermicities have equal or slightly lower values. These relative results can be understood in light of the fact that the magnitudes of the theoretical collision cross sections using these models are $\sigma_{LD} > \sigma_{Traj} > \sigma_{LGS}$, and one might expect the energetics using these collision models to reflect this order, although the differences in these results are too small to reach a definite conclusion. The magnitudes of the MADs for these bimolecular PST and RRKM analysis methods are comparable to that of the MAD for the model using eq 1 with rotational energy removed. This provides strong evidence that the good agreement observed between the CCID results and those using eq 1 with rotational energy removed is indeed fortuitous. Thus, the cause for the systematically higher thresholds when rotational and vibrational energy is included in eq 1 is due to a competitive shift of the thermoneutral reaction back to reactants. This analysis also demonstrates that for polyatomic reaction systems with small reaction endothermicities, as is the case in the current systems, the probability that the initial reaction complex will revert back to the reactants is significant and cannot be ignored when determining the thermochemistry from cross section measurements.

Analysis of Exothermic Reactions Including Competition. The cross sections for the exothermic ligand exchange reactions were also modeled using the PST (LD) and RRKM (LD and Traj) methods described above for the endothermic reactions.[46] Unlike the analysis for the endothermic reactions described above, the scaling factor (σ_0) for exothermic reactions was fixed at a value of 1.0 and was not allowed to vary during the analysis. Therefore, the only adjustable parameter in these methods is the reaction energetics. The one exception to this was the
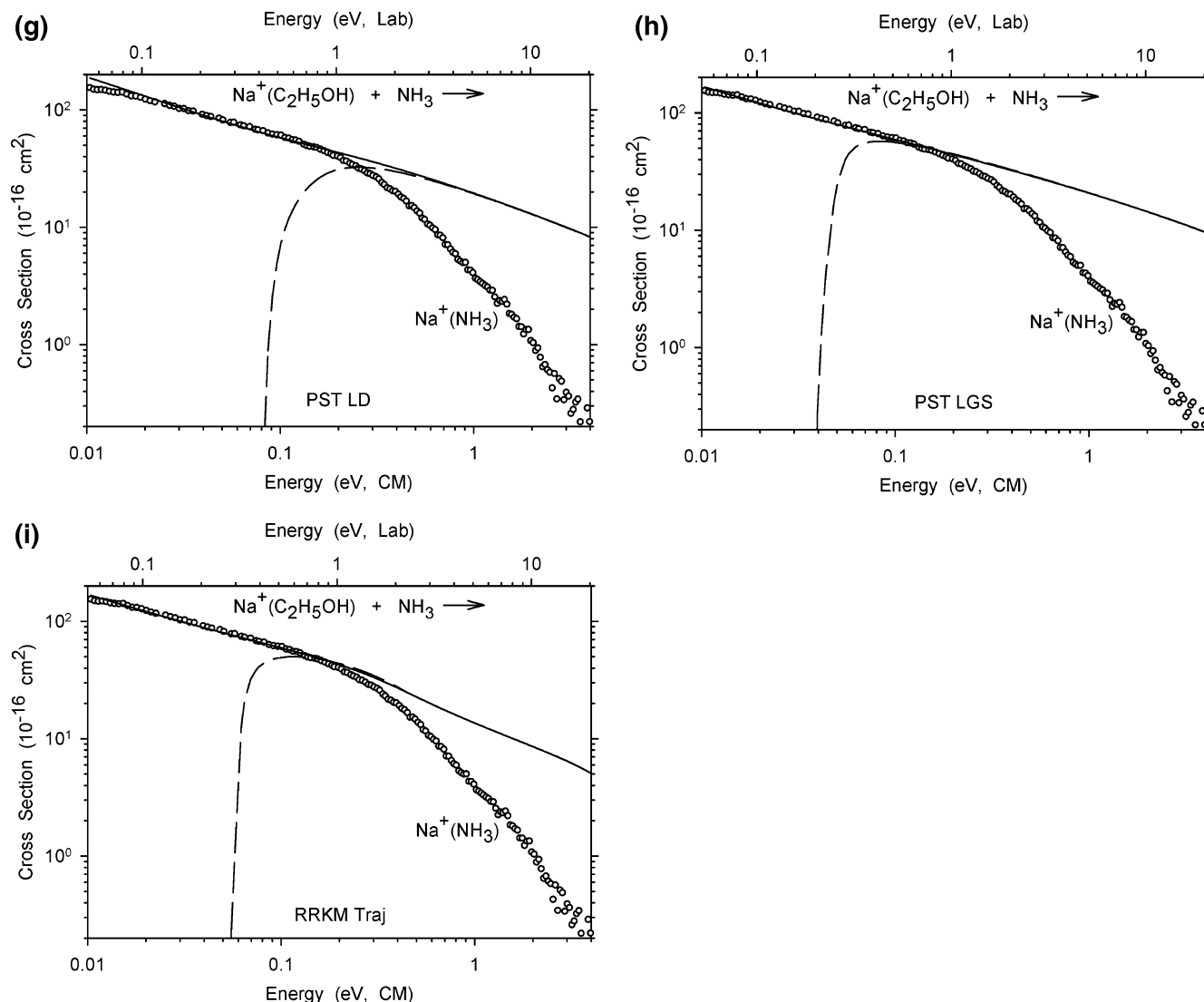
(a) Energy (eV, Lab) / Cross Section (10^{-16} cm^2) / Na$^+$(C$_2$H$_5$OH) + H$_2$O → / Na$^+$(H$_2$O) / PST LD / Energy (eV, CM)

(b) Energy (eV, Lab) / Cross Section (10^{-16} cm^2) / Na$^+$(C$_2$H$_5$OH) + H$_2$O → / Na$^+$(H$_2$O) / PST LGS / Energy (eV, CM)

(c) Energy (eV, Lab) / Cross Section (10^{-16} cm^2) / Na$^+$(C$_2$H$_5$OH) + H$_2$O → / Na$^+$(H$_2$O) / RRKM Traj / Energy (eV, CM)

(d) Energy (eV, Lab) / Cross Section (10^{-16} cm^2) / Na$^+$(ND$_3$) + CH$_3$OH → / Na$^+$(CH$_3$OH) / PST LD / Energy (eV, CM)

(e) Energy (eV, Lab) / Cross Section (10^{-16} cm^2) / Na$^+$(ND$_3$) + CH$_3$OH → / Na$^+$(CH$_3$OH) / PST LGS / Energy (eV, CM)

(f) Energy (eV, Lab) / Cross Section (10^{-16} cm^2) / Na$^+$(ND$_3$) + CH$_3$OH → / Na$^+$(CH$_3$OH) / RRKM Traj / Energy (eV, CM)

Ligand Exchange Reactions of Na$^+$ Complexes

J. Phys. Chem. A, Vol. 108, No. 48, 2004 **10707**

Figure 3. Zero-pressure-extrapolated cross sections for the endothermic ligand exchange reactions of (a−c) Na$^+$(C$_2$H$_5$OH) with H$_2$O, (d−f) Na$^+$(ND$_3$) with CH$_3$OH, and (g−i) Na$^+$(C$_2$H$_5$OH) with NH$_3$ as a function of kinetic energy in the center-of-mass frame (lower axis) and the laboratory frame (upper axis). The solid lines show the best fits to the data using the PST (LD) method in panels a, d, and g, the PST (LGS) method in panels b, e, and h, and the RRKM (Traj) method in panels c, f, and i, convoluted over the experimental kinetic energy distributions of the reactants. Dashed lines show the model cross sections in the absence of experimental kinetic energy broadening for reactants with an internal energy of 0 K.

analysis of the Na$^+$(H$_2$O) + C$_2$H$_5$OH → Na$^+$(C$_2$H$_5$OH) + H$_2$O reaction using the RRKM (Traj) method. With this reaction, the ligand exchange cross section was larger than the theoretical trajectory collision cross section, and in order to analyze the data using this method, a scaling factor of 1.4 ± 0.1 was required. We attempted to model the data using the PST (LGS) and RRKM (LGS) methods that do not include the dipole; however, for all reactions except one (Na$^+$(H$_2$O) + C$_6$H$_6$ → Na$^+$(C$_6$H$_6$) + H$_2$O), the data could not be analyzed without allowing the scaling factor to vary because the cross sections exceed the LGS limit. Because such scaling is not as satisfactory for exothermic reactions as it is for endothermic reactions, these results are not included here.

The results of the analyses of the exothermic reactions using the PST (LD) and RRKM (LD and Traj) methods are given in Table 4 along with the reaction exothermicities deduced from the CCID-determined bond energies.[8] Representative fits using the PST (LD) and RRKM (Traj) methods are displayed in Figure 4 for the Na$^+$(H$_2$O) + C$_2$H$_5$OH → Na$^+$(C$_2$H$_5$OH) + H$_2$O, Na$^+$(CH$_3$OH) + NH$_3$ → Na$^+$(NH$_3$) + CH$_3$OH, and Na$^+$(ND$_3$) + C$_2$H$_5$OH → Na$^+$(C$_2$H$_5$OH) + ND$_3$ reactions. The fits using

the RRKM (LD) method are very similar to the fits using the PST (LD) method and therefore are not displayed explicitly in Figure 4 but rather are given in Figure 9S available in the Supporting Information. For all other exothermic reactions, the fits using the PST (LD) method are given in Figure 8S, and the fits using the RRKM (LD and Traj) methods are given in Figures 9S and 10S, respectively, available in the Supporting Information.

Similar to most of the endothermic reactions, the range of energies over which the bimolecular PST and RRKM methods reproduce the data for the exothermic reactions is fairly small (0.1−0.4 eV). It is even more apparent for the exothermic reactions that the small fitting ranges and the deviations of the fits from the data at the lowest energies are related to the range of energies over which the experimental cross sections follow the scaled theoretical locked dipole and trajectory parametrization collision cross sections. Qualitatively, the PST (LD) and RRKM (LD) methods both fit the data over very similar ranges of energy and have very similar shapes. The RRKM (Traj) method, however, generally appears to fit the data over a slightly larger energy range and to a slightly lower absolute energy than

TABLE 4: Reaction Exothermicities at 0 K (eV) Obtained Using Phase Space Theory and Bimolecular RRKM Theory and Determined Using CCID Experimental Relative Bond Dissociation Energies[a]

reaction	ΔE_0			
	PST (LD)[b]	RRKM (LD)[c]	RRKM (Traj)[d]	CCID[e]
$Na^+(H_2O) + C_6H_6$	−0.03 (0.04)	−0.05 (0.04)	−0.10 (0.04)	−0.08 (0.03)
$Na^+(H_2O) + CH_3OCH_3$	−0.12 (0.05)	−0.30 (0.05)	−0.25 (0.05)	−0.13 (0.03)
$Na^+(H_2O) + C_2H_5OH$	−0.41 (0.11)	−0.52 (0.13)	−0.41 (0.08)[f]	−0.23 (0.03)
$Na^+(C_6H_6) + CH_3OH$	−0.04 (0.02)	−0.04 (0.02)	−0.07 (0.03)	−0.02 (0.02)
$Na^+(CH_3OH) + CH_3OCH_3$	−0.02 (0.03)	−0.05 (0.03)	−0.07 (0.03)	−0.03 (0.01)
$Na^+(CH_3OH) + NH_3$	−0.02 (0.02)	−0.02 (0.03)	−0.04 (0.02)	−0.05 (0.01)
$Na^+(CH_3OCH_3) + NH_3$	−0.01 (0.01)	0.00 (0.01)	−0.02 (0.01)	−0.02 (0.01)
$Na^+(ND_3) + C_2H_5OH$	−0.13 (0.03)	−0.24 (0.03)	−0.24 (0.03)	−0.10 (0.01)[g]
MAD[h]	0.04 (0.05)	0.09 (0.09)	0.07 (0.07)	
	0.02 (0.01)[i]	0.06 (0.06)[i]	0.05 (0.05)[i]	

[a] Uncertainties in parentheses. [b] Analyzed using a bimolecular, polyatomic phase space theory model and the locked dipole approximation as described in the text. [c] Analyzed using a bimolecular, competitive RRKM model and the locked dipole approximation as described in the text. [d] Analyzed using a bimolecular, competitive RRKM model and the trajectory parametrization as described in the text. [e] Reaction exothermicity obtained using relative bond dissociation energies determined by CCID experiments.[8] [f] A scaling factor (σ_0) of 1.4 ± 0.1 was used to model this reaction using the bimolecular, competitive RRKM model and the trajectory parametrization model. [g] The value has been corrected to the value for $Na^+(ND_3)$ as the reactant using zero-point energy differences of the deuterated and perprotio products and reactants (0.017 eV). [h] Mean absolute deviation from CCID-determined reaction exothermicities. [i] MAD obtained if the results for the $Na^+(H_2O) + C_2H_5OH$ reaction are excluded.

the PST (LD) or RRKM (LD) method. This is not surprising because the LD model is known to overestimate the collision cross section, whereas the Traj model should be more realistic.

Quantitatively, the agreement between the reaction exothermicities obtained from the bimolecular PST (LD) analysis and the bimolecular RRKM (LD and Traj) analyses with those determined from the CCID relative BDEs is varied. The MAD for the PST (LD) method is very good at 0.04 ± 0.05 eV (eight values); however, the MADs for both of the RRKM methods (LD and Traj) are not as satisfactory, with values of 0.09 ± 0.09 eV (eight values) and 0.07 ± 0.07 eV (eight values), respectively. An examination of Table 3 reveals that all three methods fail for the $Na^+(H_2O) + C_2H_5OH \rightarrow Na^+(C_2H_5OH)$ + H_2O reaction, with absolute deviations of +0.17, +0.27, and +0.18 eV for the PST (LD), RRKM (LD), and RRKM (Traj) methods, respectively. If these values are excluded, then the MADs improve for the remaining seven values to 0.02 ± 0.01, 0.06 ± 0.06, and 0.05 ± 0.05 eV, respectively. Even with the improved MADs, these results clearly suggest that the PST (LD) method is generally superior to either of the RRKM methods in reproducing the reaction energetics of these exothermic reactions. We suspect that the implementation of a trajectory model within a PST approach would provide even better results, but this cannot be accomplished easily because of the need to conserve angular momentum rigorously in PST.

Comparing the quantitative agreement of the methods to each other shows that for most systems the exothermicities obtained from analyses using the PST (LD) and RRKM (LD) methods are less negative than the results using the RRKM (Traj) method. Because the value of the reaction exothermicity is related to the magnitude of the cross section, the systematic difference observed is a result of the fact that the locked dipole collision cross section is larger than the trajectory parametrization collision cross section for a given polar neutral molecule. Therefore, to bring the fit using the locked dipole model close to the data, the reaction exothermicity has to be less negative compared to the value obtained using the trajectory parametrization.

Comparing to the MADs for the endothermic reactions, it can be seen that the MADs for the exothermic reactions are generally comparable to or slightly higher than those obtained for the endothermic reactions using the same methods of analysis. This is perhaps not surprising because, as mentioned

previously, the value of the reaction exothermicity obtained from the analysis of the exothermic cross sections is governed primarily by the magnitude of the cross section whereas the reaction endothermicity obtained from the analysis of an endothermic cross section is influenced primarily by the shape of the cross section. The latter constraint makes the determination of acceptable fits to the data less ambiguous and therefore more accurate. Regardless, the current results do suggest that reasonable thermochemistry can be obtained from exothermic ligand exchange reaction cross sections with careful analysis.

Thermal Rate Constants and Equilibrium Constants. From the cross section magnitudes at the lowest energies examined, thermal rate constants can be determined for the ligand exchange reactions. This was accomplished using a power law model of the energy dependence of the low-energy reaction cross sections and integrating the model using eq 2 to determine the thermal rate constants, $k(298)$, for these reactions. The power law fitting parameters and the thermal rate constants derived from these models for all of the reactions, except the $Na^+(C_2H_5OH) + H_2O \rightarrow Na^+(H_2O) + C_2H_5OH$ reaction, are listed in Table 5. For the $Na^+(C_2H_5OH) + H_2O \rightarrow Na^+(H_2O)$ + C_2H_5OH reaction, the value of the thermal rate constant was obtained by simply extrapolating the energy-dependent rate constant data, $k(\langle E \rangle)$, to an energy of 0.0385 eV (i.e., $(3/2)k_BT$ (298 K)). The rate constants obtained using the $Na^+(ND_3)$ reactant could be lower than the values for $Na^+(NH_3)$ as the reactant and may need to be corrected for the secondary isotope effect. The magnitude of the isotope effect was calculated to be $k_H/k_D = 1.25$,[60] but when the values for the reactions of $Na^+(ND_3)$ with CH_3OH, CH_3OCH_3, and C_2H_5OH were adjusted for the isotope effect, worse agreement with literature data was obtained. Hence, the adjustment is not included in the final results here. The magnitudes of the rate constants were found to vary from (8 to 29) × 10^{-10} cm³/s for the exothermic reactions and from (0.09 to 8) × 10^{-10} cm³/s for the endothermic reactions. The relative magnitudes for the forward and reverse rate constants for a particular ligand exchange reaction are found to be in accord with the reaction energetics, as described above for the relative cross section magnitudes.

Once the rate constants for the forward and reverse exchange reactions of a given pair of ligands have been determined, the equilibrium constant for the exchange reaction can be calculated from the ratio of these rate constants (i.e., $K_{LE} = k_f/k_r$, where k_f

Ligand Exchange Reactions of Na⁺ Complexes

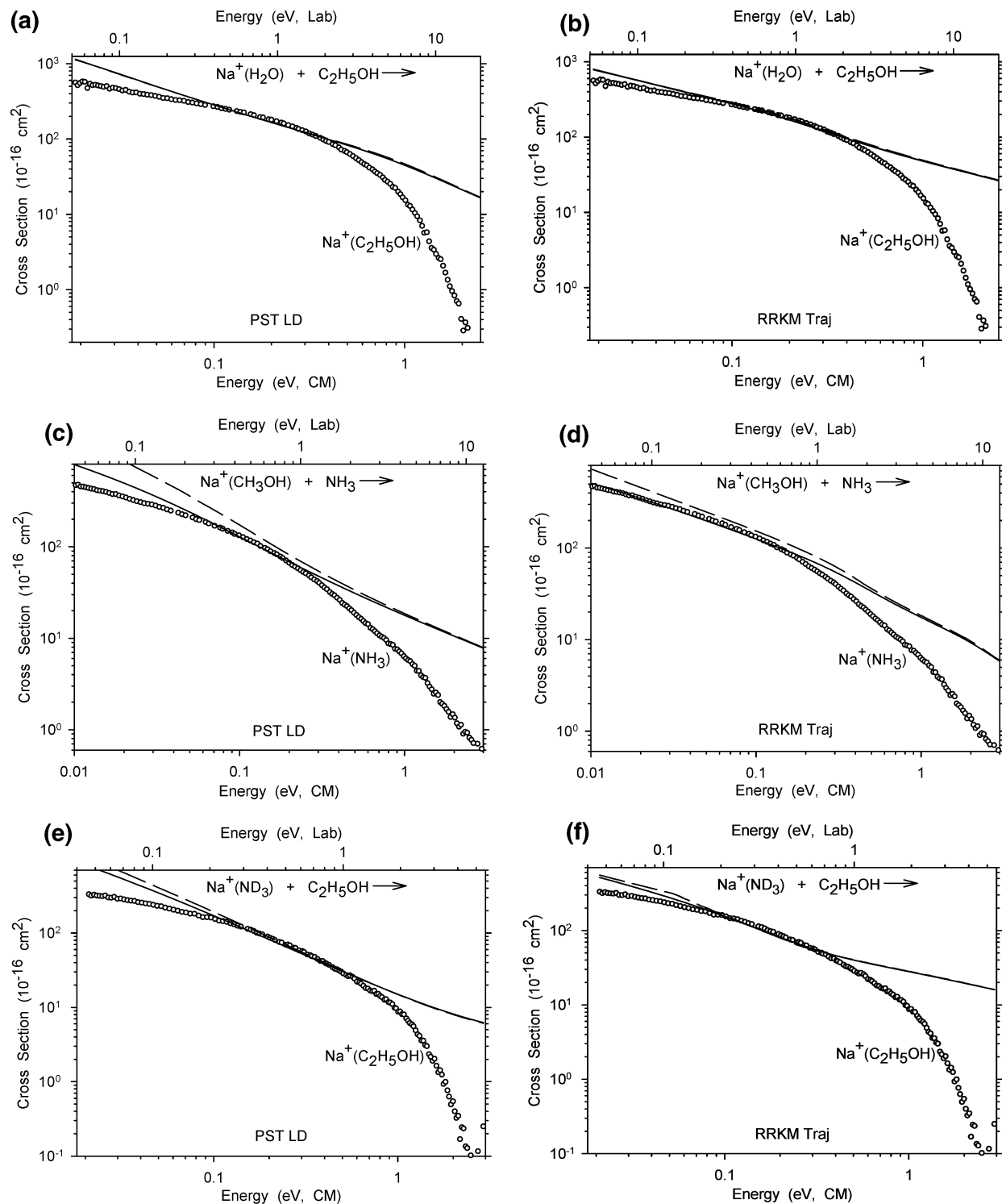*J. Phys. Chem. A, Vol. 108, No. 48, 2004* **10709**

Figure 4. Zero-pressure-extrapolated cross sections for the exothermic ligand exchange reaction of (a and b) $Na^+(H_2O)$ with C_2H_5OH, (c and d) $Na^+(CH_3OH)$ with NH_3, and (e and f) $Na^+(ND_3)$ with C_2H_5OH as a function of kinetic energy in the center-of-mass frame (lower axis) and the laboratory frame (upper axis). The solid line shows the best fit to the data using the PST (LD) method in panels a, c, and e and the RRKM (Traj) method in panels b, d, and f, convoluted over the experimental kinetic energy distributions of the reactants. The dashed line shows the model cross section in the absence of experimental kinetic energy broadening for reactants with an internal energy of 0 K.

and k_r are the forward (exothermic) and reverse (endothermic) rate constants, respectively). For the eight ligand exchange systems examined, the equilibrium constants thus determined are given in Table 5.

Relative and Absolute Na⁺−L Dissociation Free Energies. Relative 298 K free energies for the ligand exchange equilibria are listed in Table 5 and are calculated from the equilibrium

constant K_{LE} using $\Delta_{LE}G = -RT \ln(K_{LE})$, where R is the gas constant and T is the temperature in Kelvin. Table 5 also lists relative 298 K free energies determined in FT-ICR equilibrium studies.[2] As can be seen from Table 5, the agreement between the current relative free energies and the FT-ICR values is excellent, with a MAD of 0.3 ± 0.4 kJ/mol (eight values). One can also note that if the isotope corrections for the rates in the

TABLE 5: Power Law Fitting Parameters, Rate Constants (10^{-10} cm³/s), Equilibrium Constants, and Free Energies for Ligand Exchange Reactions (kJ/mol) at 298 K[a]

reaction	σ_0	m	$k(298)$	K_{LE}	$\Delta_{LE}G_{298}$	$\Delta_{LE}G_{298}$ (FT-ICR)[b]
$Na^+(H_2O) + C_6H_6$	30 (10)	0.5 (0.1)	8.1 (2.6)	1.04 (0.49)	−0.1 (1.3)	0.0 (2.0)
$Na^+(C_6H_6) + H_2O$	40 (10)	0.7 (0.1)	7.8 (2.7)			
$Na^+(H_2O) + CH_3OCH_3$	50 (10)	0.4 (0.1)	24 (10)	27 (18)	−8.1 (2.1)	−7.9 (1.8)
$Na^+(CH_3OCH_3) + H_2O$	10 (3)	0.9 (0.1)	0.9 (0.5)			
$Na^+(H_2O) + C_2H_5OH$	80 (20)	0.4 (0.1)	29 (10)	320 (210)	−14.3 (1.9)	−13.8 (1.7)
$Na^+(C_2H_5OH) + H_2O$			0.09 (0.05)[c]			
$Na^+(C_6H_6) + CH_3OH$	70 (20)	0.6 (0.1)	15 (4)	14 (6)	−6.5 (1.2)	−6.7 (1.8)
$Na^+(CH_3OH) + C_6H_6$	12 (3)	0.8 (0.1)	1.1 (0.4)			
$Na^+(CH_3OH) + CH_3OCH_3$	60 (20)	0.6 (0.1)	13 (3)	1.6 (0.6)	−1.2 (0.9)	−1.2 (1.7)
$Na^+(CH_3OCH_3) + CH_3OH$	60 (20)	0.7 (0.1)	8 (2)			
$Na^+(CH_3OH) + NH_3$	40 (10)	0.5 (0.1)	16 (5)	5.7 (2.2)	−4.3 (1.0)	−5.4 (1.6)
$Na^+(ND_3) + CH_3OH$	16 (5)	0.7 (0.1)	2.8 (0.6)			
$Na^+(CH_3OCH_3) + NH_3$	38 (9)	0.5 (0.1)	14 (3)	4.2 (1.5)	−3.6 (0.9)	−4.2 (1.6)
$Na^+(ND_3) + CH_3OCH_3$	21 (4)	0.7 (0.1)	3.3 (0.9)			
$Na^+(ND_3) + C_2H_5OH$	60 (10)	0.5 (0.1)	15 (3)	1.9 (0.6)	−1.6 (0.8)	−1.7 (1.4)
$Na^+(C_2H_5OH) + NH_3$	19 (7)	0.5 (0.1)	8 (2)			

[a] Uncertainties in parentheses. LE = ligand exchange. [b] FT-ICR equilibrium studies.[2] [c] Determined by extrapolation of the rate constant data as described in the text.

TABLE 6: Experimental Relative Na⁺−L Dissociation Free Energies at 298 K (kJ/mol), Experimental and Theoretical Absolute Na⁺−L Dissociation Free Energies at 298 K (kJ/mol), and Mean Absolute Deviations (MADs)[a]

	experiment						theory	
ligand	relative[b]	absolute[c]	FT-ICR[d]	CCID[e]	CID[f]	PHPMS[g]	MP2[h]	G2[i]
C_2H_5OH	1.7 (0.5)	79.1 (1.2)	79.5 (0.9)	79.3 (7.7)	71.4 (6.2)		78.3	77.0
NH_3	0.0	77.4 (1.1)	77.8 (1.1)	77.4 (6.6)	77.4 (6.6)	79.9 (2.6)	77.7	77.4
CH_3OCH_3	−3.5 (0.2)	73.9 (1.1)	73.6 (1.2)	74.6 (7.4)	65.7 (6.9)		75.7	74.3
CH_3OH	−4.6 (0.4)	72.8 (1.2)	72.4 (1.4)	72.4 (7.4)	66.2 (7.5)	74.8 (2.6)	74.5	73.0
C_6H_6	−11.4 (0.5)	66.0 (1.2)	65.7 (1.4)	66.5 (7.6)	63.8 (7.7)[j]		60.6	65.6
H_2O	−11.8 (0.7)	65.6 (1.4)	65.7 (1.4)	64.1 (7.4)	70.8 (8.6)		65.6	65.2
MAD[k]			0.3 (0.1)	0.6 (0.5)	5.0 (3.3)	2.3 (0.4)	1.7 (2.0)	0.6 (0.8)

[a] Uncertainties in parentheses. [b] Relative dissociation free energy, present work. [c] Absolute dissociation free energy, present work. [d] FT-ICR equilibrium studies.[2] [e] Calculated from ΔH_0 values determined from CCID[8] and enthalpy and entropy corrections determined at the MP2(full)/6-31G(d) level.[3,8] [f] Calculated from ΔH_0 values determined from direct CID[3] and enthalpy and entropy corrections determined at the MP2(full)/6-31G(d) level.[3,8] [g] Pulsed high-pressure equilibrium mass spectrometry.[1] [h] Calculated from ΔH_0 values determined at the MP2(full)/6-311+G(2d,2p)//MP2(full)/6-31G(d) level[3] and enthalpy and entropy corrections determined at the MP2(full)/6-31G(d) level.[3,8] [i] Calculated from ΔH_0 values determined using the G2 composite method[3] and enthalpy and entropy corrections determined at the MP2(full)/6-31G(d) level.[3,8] [j] ΔH_0 taken from ref 13. [k] Mean absolute deviation from present absolute ΔG_{298} values.

three systems involving $Na^+(ND_3)$ are made then the MAD increases to 0.5 ± 0.6 kJ/mol (eight values), still in good agreement with the literature.

To determine the best set of final relative free energies, incorporating all of the values from Table 5, we use a least-squares minimization of the deviations (χ^2) of the relative values from the experimental relative free energies, referenced to NH_3 as zero, using the procedure detailed by DeTuri and Ervin.[61] The final relative values are listed in Table 6. These relative free energies can then be converted to absolute 298 K dissociation free energies using an absolute dissociation free energy as an anchor value. In this work, the absolute free energies are chosen to minimize the differences with the set of values obtained from equilibrium studies of McMahon and Ohanessian using FT-ICR mass spectrometry.[2] If the differences with the set of CCID values were used instead, then all absolute values determined here would decrease by 0.1 kJ/mol.[8] The absolute free energies thus determined are presented in Table 6 and Figure 5, along with values determined from FT-ICR and pulsed high-pressure mass spectrometry (PHPMS) experiments of McMahon, Ohanessian, and co-workers.[1,2] Also included in Table 6 and Figure 5 are values derived from CCID[8] and direct CID[3] experiments in our laboratory and theoretical calculations, also performed in our laboratory,[3] at the MP2(full)/6-311+G-(2d,2p)//MP2(full)/6-31G(d) and G2[62] levels. These 298 K

dissociation free energies were obtained from the measured or calculated absolute 0 K bond energies along with entropies and enthalpy corrections calculated from molecular parameters determined at the MP2(full)/6-31G(d) level.[3,8] These theory levels were primarily chosen to be representative because of the excellent agreement that was observed between the absolute BDEs determined from our CCID experiments[8] and the theoretical BDEs calculated at these levels.[3]

As can be seen from Table 6 and Figure 5, the agreement between the present absolute dissociation free energies and five out of six types of literature values (FT-ICR, CCID, PHPMS, MP2, and G2) is excellent with MADs less than 2.3 kJ/mol. There is a larger disagreement between the current values and those derived from direct CID (MAD = 5 ± 3 kJ/mol, six values), but this just reflects the scatter in the bond energies determined from the direct CID experiments and the fact that the differences in bond energies for these ligands are, in most cases, smaller than the uncertainties of the measurements.[3,13] In general, however, the direct CID values do agree with the current ligand exchange values within the combined uncertainties of the two measurements. The excellent quantitative agreement between the ligand exchange values, those derived from CCID, and those from the FT-ICR results is particularly gratifying in that it validates the accuracy of the absolute bond
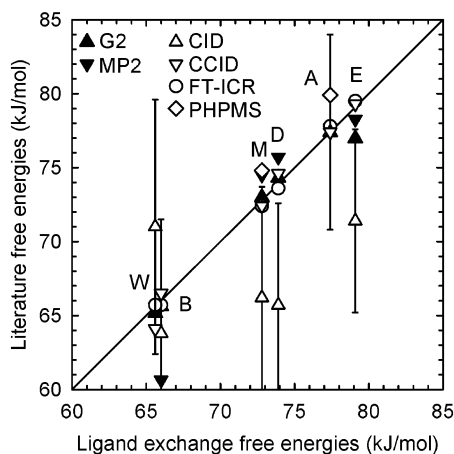
Ligand Exchange Reactions of Na$^+$ Complexes

J. Phys. Chem. A, Vol. 108, No. 48, 2004 **10711**

Figure 5. Absolute 298 K Na$^+$−L dissociation free energies determined by direct CID (open triangles with error bars),[3] CCID (open inverted triangles),[8] FT-ICR equilibrium studies (open circles),[2] pulsed high-pressure mass spectrometry equilibrium studies (PHPMS, open diamonds),[1] and theoretical calculations at the MP2(full)/6-311+G-(2d, 2p)//MP2(full)/6-31G(d) level (closed inverted triangles)[3] and using the G2 composite method (closed triangles)[3] vs ligand exchange reaction free energies determined here. All values are listed in Table 6. The diagonal line indicates values for which direct CID, CCID, FT-ICR, PHPMS, MP2, and G2 values are equal to the ligand exchange values. The designations W, B, M, D, A, and E refer to water, benzene, methanol, dimethyl ether, ammonia, and ethanol, respectively.

energies determined via the CCID experiments and the relative free energies determined here.

In terms of the order of the absolute Na$^+$−L dissociation free energies, the current experiments are in exact agreement with the order predicted in the CCID experiments, namely, ethanol > ammonia > dimethyl ether > methanol > benzene > water. The current ligand exchange experiments are in general agreement with the order predicted in the FT-ICR experiments, except that the current experiments, after averaging over all pairs, predict that the dissociation free energy of Na$^+$(C$_6$H$_6$) is slightly larger than that of Na$^+$(H$_2$O) by 0.4 kJ/mol. Within the experimental uncertainties (∼1.3 kJ/mol), however, the two values are equal, as obtained directly in the FT-ICR experiments.[2] In comparing to the theoretical calculations, there are two discrepancies. In the MP2 calculations, the water value is predicted to be 5.0 kJ/mol larger than the benzene value, which results from the inaccurate bond energy for benzene obtained with the MP2 method.[8] The discrepancy in the order predicted by the G2 calculations is that the free energy of ethanol is predicted to be slightly smaller (by 0.4 kJ/mol) than that of ammonia, whereas three experimental determinations (the current ligand exchange, FT-ICR, and CCID) and the MP2 calculations predict the opposite trend. This is primarily a result of the low G2-calculated bond energy for the ethanol ligand, 107.6 kJ/mol.[3] (Note that the cited value properly treats the ethanol internal rotors as hindered for the free ligand.)

Na$^+$−L Dissociation Entropies. Experimental dissociation entropies (Table 7) are obtained using the free energies directly determined here (Table 6) and enthalpies previously determined from CCID experiments (listed in Table 7).[8] These dissociation entropies are also compared to alternatively derived dissociation entropies in Table 7 and Figure 6. The alternate entropies are experimental values from pulsed high-pressure equilibrium mass spectrometry[1] values calculated by combining CCID bond enthalpies[8] and FT-ICR free energies[2] and theoretical entropies obtained from molecular parameters determined at the MP2-(full)/6-31G(d) level.[3,8] From Table 7 and Figure 6, it can be

seen that the agreement between the present dissociation entropies (CCID/LE) and the three types of literature values (PHPMS, CCID/FT-ICR, and MP2) is quite good, with MADs (J/K mol) of 4 ± 4 (two values), 1 ± 1 (six values), and 2 ± 2 (six values), respectively. For Na$^+$(C$_2$H$_5$OH), it is interesting that the best quantitative agreement between the two experimental values (CCID/LE and CCID/FT-ICR) and the theoretical value (MP2) is found when the methyl and hydroxy internal torsions are treated as vibrators in the complex and hindered rotors (108 J/K mol) in the neutral ethanol product, as opposed to vibrators (94 J/K mol) or free rotors (114 J/K mol) in the neutral product.[8] This result supports our hypothesis from the CCID study that the internal rotors of the neutral ethanol product in the dissociation of Na$^+$(C$_2$H$_5$OH) are most appropriately treated as hindered rotors.[8]

The present determination (CCID/LE) finds that the order of the dissociation entropies is as follows: ethanol > benzene > ammonia > dimethyl ether > methanol > water. The overall dissociation entropy for Na$^+$−L complexes comprises translational, rotational, and vibrational contributions that have a fairly complex dependence on several variables such as the masses, rotational constants, and vibrational frequencies of the species involved in the dissociation process.[63] Using the dissociation entropies calculated from the molecular parameters determined at the MP2(full)/6-31G(d) level (Table 7), some general features regarding the observed relative entropies can be understood in terms of the individual contributions. The largest contribution to the overall dissociation entropies comes from translation, 137 J/K mol for Na$^+$(NH$_3$) to 145 J/K mol for Na$^+$(C$_6$H$_6$), and these are found to increase with increasing mass of the ligand. According to this contribution, the order would be benzene > ethanol = dimethyl ether > methanol > ammonia > water. The rotational contributions to the entropies are negative values, −12 J/K mol for Na$^+$(C$_6$H$_6$) to −33 J/K mol for Na$^+$(H$_2$O), except for Na$^+$(C$_2$H$_5$OH), +13 J/K mol, and are dependent on the changes in rotational constants and symmetry numbers upon dissociation. The reason for the deviation with Na$^+$(C$_2$H$_5$OH) is that the methyl and hydroxy internal torsions are treated as hindered rotors rather than vibrators in the neutral product. The values for the vibrational contributions are also calculated to be negative, −12 J/K mol for Na$^+$(NH$_3$) to −48 J/K mol for Na$^+$(C$_2$H$_5$OH), and are generally a function of the magnitude of the metal−ligand frequencies that are lost upon dissociation. Combining these contributions leads to the order predicted using the molecular parameters obtained from the MP2(full)/6-31G-(d) calculations (Table 7): ethanol > benzene > ammonia > methanol = water > dimethyl ether. In general, these calculations qualitatively predict the overall trends in the entropies as compared to the experimentally determined values (CCID/LE), except for the dimethyl ether system, with the calculations predicting a lower value than those for methanol and water. In light of this discrepancy, it was also considered whether the methyl torsions for dimethyl ether and methanol should be treated as hindered rotors rather than vibrators for both the complex ion and the neutral products in the dissociation reactions. When using a hindered rotor treatment, the dissociation entropies are predicted to be 91.5 and 89.8 J/K mol for dimethyl ether and methanol, respectively. These values agree better with the experimental values. Using these corrected dissociation entropies, the order predicted using the MP2(full)/6-31G(d) calculated molecular parameters is ethanol > benzene > ammonia > dimethyl ether > water ≈ methanol, in good agreement with the CCID/LE and CCID/FT-ICR orders.

TABLE 7: Absolute Na$^+$–L Bond Dissociation Enthalpies (in kJ/mol) and Na$^+$–L Dissociation Entropies (in J/K mol)[a]

ligand	ΔH_{298}[b] CCID	ΔS			
		CCID/LE[c]	CCID/FT-ICR[d]	PHPMS[e]	MP2[f]
C_2H_5OH	111.4 (5.6)	108 (19)	107 (19)		108[g]
NH_3	106.2 (5.7)	97 (19)	95 (19)	91 (8)	97
CH_3OCH_3	101.4 (5.6)	92 (19)	93 (19)		90 (92[h])
CH_3OH	98.8 (5.7)	87 (19)	88 (20)	86 (8)	91 (90[h])
C_6H_6	97.0 (5.9)	104 (20)	105 (20)		102
H_2O	91.2 (6.3)	86 (22)	86 (22)		91
MAD[i]			1 ± 1	4 ± 4	2 ± 2 (2 ± 2)

[a] Uncertainties in parentheses. [b] CCID.[8] [c] Determined by combining CCID ΔH_{298} values[8] with ligand exchange (LE) ΔG_{298} values (column 3, Table 6). [d] Determined by combining CCID ΔH_{298} values[8] with FT-ICR ΔG_{298} values (column 4, Table 6).[2] [e] Pulsed high-pressure equilibrium mass spectrometry.[1] [f] Calculated using standard formulas and molecular parameters determined at the MP2(full)/6-31G(d) level.[3,8] [g] Calculated treating the methyl and hydroxy internal rotors of the neutral ethanol product as hindered rotors.[8] [h] Calculated treating the methyl internal rotors of the complex ion and the neutral products as hindered rotors.[8] [i] Mean absolute deviation from CCID/LE ΔS values.
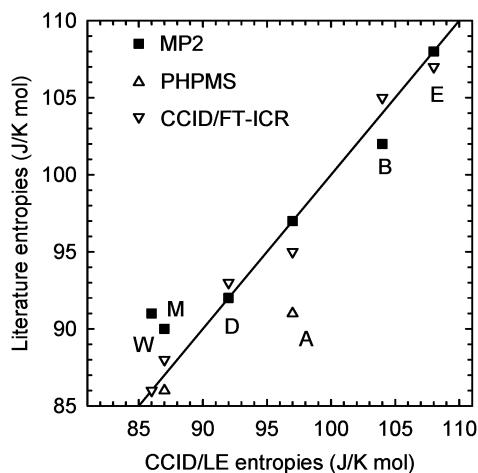

Figure 6. Dissociation entropies determined experimentally by pulsed high-pressure equilibrium mass spectrometry (PHMS, open triangles)[1] and by combining FT-ICR ΔG_{298} values[2] with CCID ΔH_{298} values[8] (CCID/FT-ICR, open inverted triangles) and theoretically using standard formulas and molecular parameters determined at the MP2(full)/6-31G-(d) level[3,8] (MP2, closed squares) vs dissociation entropies determined by combining CCID ΔH_{298} values[8] with ligand exchange ΔG_{298} values (CCID/LE, present work). All values are listed in Table 7. The diagonal line indicates values for which PHPMS, CCID/FT-ICR, and MP2 values are equal to the CCID/LE values. The designations W, B, M, D, A, and E refer to water, benzene, methanol, dimethyl ether, ammonia, and ethanol, respectively.

Conclusions

The kinetic energy dependences of ligand exchange reactions of Na$^+$L$_1$ with L$_2$, where L$_1$, L$_2$ = H$_2$O, C$_6$H$_6$, CH$_3$OH, CH$_3$OCH$_3$, NH$_3$, and C$_2$H$_5$OH, are studied using guided ion beam mass spectrometry. Reaction endothermicities obtained from the endothermic ligand exchange reactions, using our empirical threshold modeling equation, are found to be systematically higher than values determined using CCID experiments[8] by 0.07–0.2 eV. An analysis of the endothermic cross sections using bimolecular, polyatomic PST methods with the LD and LGS models and competitive, bimolecular RRKM methods with the LD, Traj, and LGS models demonstrates that the systematic deviations result from a competitive shift between the thermoneutral reaction back to reactants and the endothermic reaction to the ligand exchange products. The reaction endothermicities thus obtained using the various PST (LD and LGS) and RRKM (LD, Traj, and LGS) analyses are found be in very good agreement with those determined using CCID experiments, with MADs of 0.03, 0.04, 0.03, 0.04, and 0.04 eV, respectively. Reaction exothermicities are also obtained by modeling the exothermic ligand exchange cross sections using the bimolecu-

lar, polyatomic PST(LD) and the competitive, bimolecular RRKM (LD and Traj) methods. These are found to be in general agreement with those determined using CCID experiments, with MADs of 0.04, 0.09, and 0.07 eV, respectively, if the results from all reactions are included and 0.02, 0.06, and 0.05 eV, respectively, if the results from the Na$^+$(H$_2$O) + C$_2$H$_5$OH → Na$^+$(C$_2$H$_5$OH) + H$_2$O reaction are not included. By comparison of the MADs, the PST (LD) method was deemed to be the best method for analyzing exothermic reactions, although it is surmised that being able to implement a trajectory estimate of the collision cross section within the rigorous angular momentum conservation of the PST model would lead to further improvements.

For all ligand exchange reactions, thermal rate constants, k(298), are determined from the low-energy portions of the cross sections. Using the rate constants for the forward (exothermic) and reverse (endothermic) reactions, equilibrium constants and relative dissociation free energies at 298 K are obtained. The relative Na$^+$–L free energies are converted to absolute dissociation free energies by minimizing the deviations with the ΔG_{298} values determined previously by McMahon and Ohanessian.[2] Comparisons are made to previous experimental and theoretical dissociation free energies, and the agreement between the current values and the literature values is excellent, with MADs generally below ±2.3 kJ/mol.

Using the free energies determined in this study and bond enthalpies determined from our previous CCID study,[8] Na$^+$–L dissociation entropies have been obtained. When compared to the available experimental and theoretical literature entropies, the agreement was good, with MADs below ±4 J/K mol. For Na$^+$(C$_2$H$_5$OH), the best agreement between the experimental and theoretical entropies was obtained when the methyl and hydroxy internal torsions were treated as vibrators in the complex and hindered rotors in the neutral product, verifying that this is the most appropriate treatment. Some indication is also found that dimethyl ether and methanol should be treated as hindered rotors in the complex and neutral product.

Supporting Information Available: Combined with the figures included in the paper, the 10 figures in the Supporting Information show all reaction systems studied and all variations of the modeling, as discussed in the text. This material is available free of charge via the Internet at http://pubs.acs.org.

Ligand Exchange Reactions of Na$^+$ Complexes

J. Phys. Chem. A, Vol. 108, No. 48, 2004 **10713**

References and Notes

(1) Hoyau, S.; Norrman, K.; McMahon, T. B.; Ohanessian, G. *J. Am. Chem. Soc.* **1999**, *121*, 8864−8875.

(2) McMahon, T. B.; Ohanessian, G. *Chem.−Eur. J.* **2000**, *6*, 2931−2941.

(3) Armentrout, P. B.; Rodgers, M. T. *J. Phys. Chem. A* **2000**, *104*, 2238−2247.

(4) Rodgers, M. T.; Armentrout, P. B. *Mass Spectrom. Rev.* **2000**, *19*, 215−247.

(5) Kish, M. M.; Ohanessian, G.; Wesdemiotis, C. *Int. J. Mass Spectrom.* **2003**, *227*, 509−524.

(6) Lippard, S. J.; Berg, J. M. *Principles of Bioinorganic Chemistry*; University Science Books: Mill Valley, CA, 1994.

(7) Liao, P. C.; Allison, J. *J. Mass Spectrom.* **1995**, *30*, 408.

(8) Amicangelo, J. C.; Armentrout, P. B. *Int. J. Mass Spectrom.* **2001**, *212*, 301−325.

(9) Guo, B. C.; Purnell, J. W.; Castleman, A. W., Jr. *Chem. Phys. Lett.* **1990**, *168*, 155.

(10) Dzidic, I.; Kebarle, P. *J. Phys. Chem.* **1970**, *74*, 1466−1474.

(11) Gilligan, J. J.; McCunn, L. R.; Leskiw, B. D.; Herman, Z.; Castleman, A. W., Jr. *Int. J. Mass Spectrom.* **2001**, *204*, 247−253.

(12) Dalleska, N. F.; Tjelta, B. L.; Armentrout, P. B. *J. Phys. Chem.* **1994**, *98*, 4191−4195.

(13) Amicangelo, J. C.; Armentrout, P. B. *J. Phys. Chem. A* **2000**, *104*, 11420−11432.

(14) Ervin, K. M.; Armentrout, P. B. *J. Chem. Phys.* **1985**, *83*, 166−189.

(15) Schultz, R. H.; Armentrout, P. B. *Int. J. Mass Spectrom. Ion Processes* **1991**, *107*, 29−48.

(16) Muntean, F.; Armentrout, P. B. *J. Chem. Phys.* **2001**, *115*, 1213−1228.

(17) Teloy, E.; Gerlich, D. *Chem. Phys.* **1974**, *4*, 417−427.

(18) Gerlich, D. In *State-Selected and State-to-State Ion−Molecule Reaction Dynamics, Part 1: Experiment*; Ng, C. Y., Baer, M., Eds.; John Wiley & Sons: New York, 1992; Vol. LXXXII, pp 1−176.

(19) Loh, S. K.; Lian, L.; Hales, D. A.; Armentrout, P. B. *J. Chem. Phys.* **1988**, *89*, 3378−3379.

(20) Schultz, R. H.; Crellin, K. C.; Armentrout, P. B. *J. Am. Chem. Soc.* **1991**, *113*, 8590−8601.

(21) Dalleska, N. F.; Honma, K.; Sunderlin, L. S.; Armentrout, P. B. *J. Am. Chem. Soc.* **1994**, *116*, 3519−3528.

(22) Dalleska, N. F.; Honma, K.; Armentrout, P. B. *J. Am. Chem. Soc.* **1993**, *115*, 12125−12131.

(23) Khan, F. A.; Clemmer, D. E.; Schultz, R. H.; Armentrout, P. B. *J. Phys. Chem.* **1993**, *97*, 7978−7987.

(24) Schultz, R. H.; Armentrout, P. B. *J. Chem. Phys.* **1992**, *96*, 1046−1052.

(25) Fisher, E. R.; Kickel, B. L.; Armentrout, P. B. *J. Phys. Chem.* **1993**, *97*, 10204−10210.

(26) Rodgers, M. T.; Armentrout, P. B. *J. Phys. Chem. A* **1999**, *103*, 4955−4963.

(27) Beyer, T. S.; Swinehart, D. F. *Commun. ACM* **1973**, *16*, 379.

(28) Stein, S. E.; Rabinovich, B. S. *Chem. Phys. Lett.* **1977**, *49*, 1883.

(29) Pople, J. A.; Schlegel, H. B.; Raghavachari, K.; DeFrees, D. J.; Binkley, J. F.; Frisch, M. J.; Whitesides, R. F.; Hout, R. F.; Hehre, W. J. *Int. J. Quantum Chem. Symp.* **1981**, *15*, 269.

(30) DeFrees, D. J.; McLean, A. D. *J. Chem. Phys.* **1985**, *82*, 333.

(31) Chesnavich, W. J.; Bowers, M. T. *J. Phys. Chem.* **1979**, *83*, 900−905.

(32) Armentrout, P. B. In *Advances in Gas-Phase Ion Chemistry*; Adams, N. G., Babcock, L. M., Eds.; JAI Press: Greenwich, CT, 1992; Vol. 1, pp 83−119.

(33) Rodgers, M. T.; Armentrout, P. B. *J. Phys. Chem. A* **1997**, *101*, 2614−2625.

(34) More, M. B.; Glendening, E. D.; Ray, D.; Feller, D.; Armentrout, P. B. *J. Phys. Chem.* **1996**, *100*, 1605−1614.

(35) Ray, D.; Feller, D.; More, M. B.; Glendening, E. D.; Armentrout, P. B. *J. Phys. Chem.* **1996**, *100*, 16116−16125.

(36) More, M. B.; Ray, D.; Armentrout, P. B. *J. Phys. Chem. A* **1997**, *101*, 831−839.

(37) Rodgers, M. T.; Armentrout, P. B. *J. Phys. Chem. A* **1997**, *101*, 1238−1249.

(38) More, M. B.; Ray, D.; Armentrout, P. B. *J. Phys. Chem. A* **1997**, *101*, 4254−4262.

(39) More, M. B.; Ray, D.; Armentrout, P. B. *J. Phys. Chem. A* **1997**, *101*, 7007−7017.

(40) Chantry, P. J. *J. Chem. Phys.* **1971**, *55*, 2746.

(41) Lifshitz, C.; Wu, R. L. C.; Tiernan, T. O.; Terwillger, D. T. *J. Chem. Phys.* **1978**, *68*, 247.

(42) Armentrout, P. B.; Simons, J. *J. Am. Chem. Soc.* **1992**, *114*, 8627−8633.

(43) Chesnavich, W. J.; Bowers, M. T. *J. Phys. Chem.* **1977**, *66*, 2306.

(44) Webb, D. A.; Chesnavich, W. J. *J. Phys. Chem.* **1984**, *87*, 3791.

(45) Rodgers, M. T.; Armentrout, P. B. *J. Chem. Phys.* **1998**, *109*, 1787−1800.

(46) Koizumi, H.; Armentrout, P. B. *J. Chem. Phys.* **2003**, *119*, 12819−12829.

(47) Koizumi, H.; Muntean, F.; Armentrout, P. B. *J. Chem. Phys.* **2004**, *120*, 756−766.

(48) Moran, T. F.; Hammill, W. H. *J. Chem. Phys.* **1963**, *39*, 1413.

(49) Iceman, C.; Armentrout, P. B. *Int. J. Mass Spectrom.* **2003**, *222*, 329−349.

(50) Su, T. *J. Chem. Phys.* **1994**, *100*, 4703.

(51) Gioumousis, G.; Stevenson, D. P. *J. Chem. Phys.* **1958**, *29*, 292.

(52) Rothe, E. W.; Bernstein, R. B. *J. Chem. Phys.* **1959**, *31*, 1619−1627.

(53) Applequist, J.; Carl, J. R.; Fung, K. K. *J. Am. Chem. Soc.* **1972**, *94*, 2952−2960.

(54) McClellan, A. L. *Experimental Table of Dipole Moments*; W. H. Freeman: San Francisco, CA, 1963.

(55) Tjelta, B. L.; Walter, D.; Armentrout, P. B. *Int. J. Mass Spectrom.* **2001**, *204*, 7−21.

(56) Weber, M. E.; Elkind, J. E.; Armentrout, P. B. *J. Chem. Phys.* **1986**, *84*, 1521−1529.

(57) DeTuri, V. F.; Su, M. A.; Ervin, K. M. *J. Phys. Chem. A* **1999**, *103*, 1468−1479.

(58) Ervin, K. M.; Armentrout, P. B. *J. Chem. Phys.* **1987**, *86*, 2659−2673.

(59) Ervin, K. M.; Armentrout, P. B. *J. Chem. Phys.* **1986**, *84*, 6738−6749.

(60) Lowry, T. H.; Richardson, K. S. *Mechanism and Theory in Organic Chemistry*, 3rd ed.; HarperCollins: New York, 1987.

(61) DeTuri, V. F.; Ervin, K. M. *J. Phys. Chem. A* **1999**, *103*, 6911−6920.

(62) Curtiss, L. A.; Raghavachari, K.; Trucks, G. W.; Pople, J. A. *J. Chem. Phys.* **1991**, *94*, 7221.

(63) McQuarrie, D. A. *Statistical Thermodynamics*; University Science Books: Mill Valley, CA, 1973.